Published in final edited form as:

Ultrasound Med Biol. 2020 February ; 46(2): 193–215. doi:10.1016/j.ultrasmedbio.2019.09.011.

Sonobactericide: An emerging treatment strategy for bacterial infections

Kirby R. Lattwein[a], **Himanshu Shekhar**[b], **Joop J.P. Kouijzer**[a], **Willem J.B. van Wamel**[c], **Christy K. Holland**[b], **Klazina Kooiman**[a]

[a]Department of Biomedical Engineering, Thoraxcenter, Erasmus MC, University Medical Center Rotterdam, Rotterdam, the Netherlands

[b]Department of Internal Medicine, Division of Cardiovascular Health and Disease, University of Cincinnati, Cincinnati, Ohio, USA

[c]Department of Medical Microbiology and Infectious Diseases, Erasmus MC, University Medical Center Rotterdam, Rotterdam, the Netherlands

Abstract

Ultrasound has been developed as both a diagnostic tool and a potent promoter of beneficial bioeffects for the treatment of chronic bacterial infections. Bacterial infections, especially ones involving biofilm on implants, indwelling catheters, and heart valves, affect millions of people each year and many deaths occur as a consequence. Ultrasound exposure of microbubbles or droplets can directly affect bacteria and enhance efficacy of antibiotics or other therapeutics, which we have termed *sonobactericide*. The present review summarizes investigations that have provided evidence for ultrasound-activated microbubble or droplet treatment of bacteria and biofilm. In particular, we review the type of bacteria and therapeutics used for treatment, and the *in vitro* and pre-clinical experimental set-ups employed in sonobactericide research. Mechanisms for ultrasound enhancement of sonobactericide, with a special emphasis on acoustic cavitation and radiation force are reviewed, and the potential for clinical translation is discussed.

Keywords

antibiotic; bacteria; biofilm; contrast agents; infection; microbubbles; nanodroplet; sonobactericide; ultrasound

INTRODUCTION

Over the last decades, the combination of ultrasound and cavitation nuclei has been investigated as an alternative approach to treat several life-threatening diseases. Ultrasound

Correspondence: Kirby R. Lattwein, Thoraxcenter Biomedical Engineering, Room Ee2302, Erasmus MC, University Medical Center Rotterdam, P.O.Box 2040, 3000 CA Rotterdam, the Netherlands, k.lattwein@erasmusmc.nl; Phone: +31-10-7044633.

is a common diagnostic tool and offers several advantages, including noninvasive, inexpensive, point-of-care, and safe medical applications. Many different types of cavitation nuclei exist, which can be gas or liquid filled and coated or non-coated. This includes micro- and nano-bubbles, nanocups, droplets, and echogenic liposomes. When exposed to ultrasound pressure waves, gas-filled nuclei respond by expanding and contracting volumetrically and droplets vaporize into microbubbles. Microbubble oscillations and acoustic droplet vaporization impart theragnostic potential because this characteristic response can both be detected by clinical diagnostic ultrasound scanners and locally enhance treatment by inducing cellular responses (Sutton, et al. 2013, Kooiman, et al. 2014, Wang, et al. 2018). “Sonobactericide” describes the enhancement of bactericidal action aided by ultrasound and the presence of cavitation nuclei, both endogenous and exogenous. This terminology is consistent with the nomenclature of other therapeutic applications of ultrasound-activated cavitation nuclei such as sonoporation – the formation of micropores within cell membranes (Kooiman, et al. 2014), sonothrombolysis – the lysis of thrombi (Sutton, et al. 2013), sonoreperfusion – the restoration of perfusion after micro-vascular obstruction (Black, et al. 2016), and sonodynamic therapy – the treatment of neoplastic cells using a sonosensitizer (Rosenthal, et al. 2004). Sonobactericide, just like the other approaches, can be used either alone or in combination with other drugs, such as antimicrobials.

Sonobactericide arrives at a time when traditional microbial therapy is limited by the increasing prevalence of multidrug-resistant bacteria. There are several resistance mechanisms and a large contributing factor is the development of biofilms, bacterial communities encased in a complex extracellular polymeric matrix consisting of variable amounts of numerous constituents, such as polysaccharides and proteins. This matrix provides both a scaffold for antibiotic binding and an anoxic and acidic environment that can deactivate antibiotics and decrease bacterial susceptibility via a reduced metabolism (Algburi, et al. 2017). In addition to the presence of a protective extracellular matrix, the large heterogeneity and general three-dimensional structure of a biofilm hinders antibiotic delivery penetration, and effectiveness. Additionally, it is difficult to diagnose bacterial infections before they become extensively established (Grant and Hung 2013, Werdan, et al. 2014). Sonobactericide, as illustrated in Figure 1, may increase the “footprint” of antibiotic bactericidal action, directly kill bacteria, and reduce treatment time.

This review focuses specifically on the principles of sonobactericide using exogenous cavitation nuclei for potential clinical translation. As this new line of research gains ground, it is pertinent to establish important considerations for future work. Main concepts of the variability of bacteria, microbubble composition and acoustic behavior, and ultrasound parameters are addressed, and the experimental set-ups and measured outcomes are evaluated. Articles on sonobactericide published before August 2019 were identified using Pubmed, Web of Science, and Google Scholar search engines with the keywords, “ultrasound”, “microbubble” (or “bubble” or “contrast”), and “bacteria” or “biofilm”. Sonobactericide articles referenced by those found in our search were also included. Articles were excluded if they were not written in English or if ultrasound alone, i.e. without added cavitation nuclei (i.e. microbubbles or droplets), was investigated as a potential application for treatment. For treatment with ultrasound alone, the reader is referred to other excellent

reviews (Erriu, et al. 2014, Cai, et al. 2017, Vyas, et al. 2019). Twenty-seven sonobactericide articles were selected for this review, see Table 1. One article that investigated targeted microbubbles to biofilm for diagnostic application (Anastasiadis, et al. 2014) and six articles that studied the effect of cavitation nuclei on bacteria without ultrasound (Cavalieri, et al. 2008, Cavalieri, et al. 2012, Zhou, et al. 2012, Cavalieri, et al. 2013, Mahalingam, et al. 2015, Argenziano, et al. 2017) were excluded from Table 1 because these studies did not meet our definition of sonobactericide.

BACTERIA

There exists a vast diversity among bacteria, even closely related bacteria can have different morphologies, metabolisms, and defenses. Considering shape morphology, besides the familiar rod (bacillus), spherical (coccus), and spiral (twisted) types, at least six other general shapes exist (Kysela, et al. 2016). Though current sonobactericide research into pathogenic bacteria is dominated by bacilli- and cocci-shaped bacteria, infectious diseases are also caused by bacteria with other morphologies. Microbubbles may oscillate differently when paired with similarly spherical-shaped *Staphylococcus aureus*, versus rod-shaped *Escherichia coli*, or the junction of kidney-shaped diplococci *Neisseria meningitidis* due to total surface area contact, tension, and rigidity. These shape differences along with variation in cell surface could influence treatment success. For example, fimbriae are bristle-like external filamentous structures protruding from some bacterial cell surfaces which may create a stand-off distance between the cavitation nuclei and cell wall. It has been observed that as the initial stand-off distance increases, biofilm disruption, sonoporation, and cytoskeleton disassembly decrease (Goh, et al. 2015, Wang, et al. 2018). Moreover, microbubble dynamics also depend on the distance from and material properties of a surface (Overvelde, et al. 2011, Rooij, et al. 2017).

Based on the cell envelope (a multilayered structure on the outside of the cell) almost all bacteria can be subdivided in two main groups: Gram+ or Gram−. The cell envelope of Gram+ bacteria consists of a thick (20–80 nm) peptidoglycan layer, which is threaded with teichoic acid, but lacks an outer membrane as illustrated in Figure 2A. Peptidoglycan is made up of repeating units of muramic acid, which are cross-linked by peptide side chains. Gram− bacteria are covered by a thin peptidoglycan cell wall (<10 nm), surrounded by an outer lipid bilayer membrane containing pores, lipoproteins, and lipopolysaccharide (Silhavy, et al. 2010) as illustrated in Figure 2B. It is possible that these structural differences between Gram+ and Gram− bacteria will also result in a dissimilar response to sonobactericide. Several studies have compared treatment efficacy on both bacteria types (Mai-Prochnow, et al. 2016), including ultrasound (67 and 20 kHz) paired with antibiotics without exogenous cavitation nuclei (Pitt, et al. 1994, Liao, et al. 2018), and demonstrated a markedly different response. Furthermore, the size of the bacteria (~0.5–5 μm), whether it's a single bacterium, dividing bacterium, or aggregates of several bacteria, and its location (in a suspension, on a surface, or intracellular) could have an impact on the therapeutic effectiveness of sonobactericide.

Seemingly subtle differences within a group of eukaryote cells can affect the differential reaction to oscillating microbubbles. This variable cell response to microbubbles is

supported by sonoporation studies which have demonstrated differences in drug delivery efficiency in two different cancer cell lines (Escoffre, et al. 2011). The top three types of bacteria where sonobactericide has been evaluated are 1) *Staphylococcus epidermidis* (Gram+, seven studies; 26%); 2) *S. aureus* (Gram+, six studies; 22%); and 3) *E. coli* (Gram−, four studies; 15%) (Table 1). Methicillin resistant *S. epidermidis* was employed in the majority of the studies (six out of seven), whereas for methicillin resistant *S. aureus* (MRSA) this was four out of the six studies. Two research teams used a green fluorescent protein containing Gram− strain (*E. coli*, *Pseudomonas aeruginosa*) (Tandiono, et al. 2012, Ronan, et al. 2016). The majority of the studies used only one type of bacteria. Only one study used mixed types of bacteria (Agarwal, et al. 2014). Two articles compared two different types of bacteria (Zhu, et al. 2013, Li, et al. 2015), and another compared a bacteria and a fungus (Tandiono, et al. 2012). Only four studies used patient-derived clinical isolates originating from a central venous catheter (Hu, et al. 2018), infective endocarditis blood culture (Lattwein, et al. 2018), pneumonia-induced sputum (Fu, et al. 2019), and urine from a patient with lower urinary tract symptoms (Horsley, et al. 2019). With the exception of Agarwal et al. (2014), who used bacteria from a wastewater reclamation plant for investigating membrane biofouling removal, the other groups used lab-derived strains, which may limit clinical applicability. Though a laboratory strain may be deemed wild-type, the preparation and (world-wide) dissemination can lead to genetic changes that cause both disruption of virulence regulatory pathways, which often imparts loss of typical *in vivo* virulence potential, and phenotypic variation among an entire strain pedigree (Bæk, et al. 2013). Also, typing clinical isolates, such as staphylococcal protein A (*spa*) typing performed by Lattwein et al. (2018) or core-genome multi-locus sequence typing (MLST+), would aid in the verification of disease association.

Three modes of growth exist for bacteria: planktonic, associated with a surface, or intracellular. Bacteria in different growth modes have distinctly different characteristics. Planktonic refers to free living bacterial cells which can occur in two forms: single bacterial cells or in clusters known as planktonic aggregates (Crosby, et al. 2016). Clinically, this planktonic mode generally refers to bacteria that gain entrance to the human body in the bloodstream leading to bacteremia, which causes acute infections often effectively treated by the host immune system and antibiotics (Stewart and William Costerton 2001, Brady, et al. 2018). Seven sonobactericide studies (26%) focused on planktonic bacteria (Table 1).

In contrast, bacteria adhering to living (biotic) and nonliving (abiotic) surfaces cover themselves with a protective matrix, classically known as a biofilm. Bacteria in a biofilm are protected against attacks from the immune system and are up to 1000 times more resistant to antimicrobial therapy than planktonic bacteria (Lewis 2005). Biofilm formation is abundant and an estimated 60% of human bacterial infections are biofilm related (Costerton, et al. 1999, Fux, et al. 2003). Correspondingly, 63% (17/27) of the sonobactericide studies focused on treatments for biofilm infections. Biofilm can occur on teeth, native and prosthetic heart valves, medical implants, such as prosthetic joints, surgical mesh and screws, pacemakers, and indwelling catheters (Lebeaux, et al. 2014). These biofilms consist of surface aggregates of bacteria imbedded in an extracellular matrix of sugars from bacterial origin, extracellular DNA and proteins, both originating from either the host or the bacteria. For instance, when *S. aureus* is exposed to blood, the coagulation cascade is

activated by coagulase produced by the bacterium. The fibrin forms a scaffold to which the bacteria bind, facilitating the formation of a biofilm (Zapotoczna, et al. 2016). Other biofilm composition examples include *P. aeruginosa* forming sputum-encased biofilms surrounded by immune cells in cystic fibrosis lungs (Maurice, et al. 2018), and *Proteus mirabilis* forming crystalline biofilms by inducing urinary salt precipitation in the catharized urinary tract (Delcaru, et al. 2016). Biofilm extracellular matrix composition and architecture is complex and highly influenced by species/strain/lineage, developmental conditions, nutrient availability, cell-cell signaling, and interactions with the (host) environment (Magana, et al. 2018). Moreover, most biofilm infections are polymicrobial (Short, et al. 2014), which further adds to the microenvironment complexity. The various processes driving bacterial responses are not completely understood. Thus simulating human *in vivo* biofilms remains highly challenging (Bjarnsholt, et al. 2013, Roberts, et al. 2015).

There are indications that bacteria in a single biofilm do not behave “en groupe.” Archer et al. (2011) found that *S. aureus* biofilms contain cells in at least four distinct metabolic states: aerobic, fermentative, dormant (including very slow growing cells and persisters), or dead. It is likely that bacterial cells in different metabolic states, stages of cell division, or growth phases will respond differently to sonobactericide. This hypothesis is supported by the observation that planktonic bacteria in stationary growth phase are more resistant to both ultrasound alone or combined with cavitation nuclei (Vollmer, et al. 1998).

Bacteria can disperse from mature biofilms and become planktonic again (Otto 2008). Dispersal agents, including chemical, enzymatic, and mechanical methods, can also be used to make biofilm bacteria more susceptible to therapeutics. Recent literature on *P. aeruginosa* suggests that bacteria dispersed from biofilms have a different physiology than those of both planktonic and biofilm growth modes (Chua, et al. 2014). This difference suggests a possible transitional growth mode for bacteria acclimatizing to the planktonic state. These researchers found that the dispersed cell phenotype was highly virulent and remained for at least 2 h. This finding is supported further by studies that manipulated biofilm dispersal, which led to increased disease severity and progression in mice and a transition from asymptomatic colonization to active infection, respectively (Connolly, et al. 2011, Marks, et al. 2013). Chau et al. (2014) also discovered that dispersed cells exhibited lower iron uptake gene expression and paired the dispersal agent with an iron-chelator, which led to significant reduced viability. Other work demonstrated that dispersed bacteria exhibited increased antibiotic susceptibility and only after lag phase (≥ 3 h) were more active (Lee, et al. 2018). Thus, biofilm dispersal should be considered and investigated for sonobactericide development.

EXPERIMENTAL APPROACHES

The first group to report sonobactericide in combination with an antimicrobial was Ikeda-Dantsuji et al. in 2011. Since then, 18 sonobactericide papers have been published using antimicrobials (Table 1). The most studied clinical antibiotic was vancomycin (seven studies, 26%). Six other antibiotics were investigated, with different ones for Gram+ and Gram− bacteria except gentamicin. Two groups investigated two antibiotics separately on the same bacterial strain. Ikeda-Dantsuji, et al. (2011) investigated one antibiotic to which the *C.*

trachomatis strain was susceptible (doxycycline) and one to which this bacterial strain was resistant (ceftizoxime). Ronan et al. (2016) used two aminoglycosides (gentamicin and streptomycin) to which the *P. aeruginosa* PAO1 strain was susceptible determined by CO_2 metabolic production.

Besides antibiotics, three other antimicrobials were investigated: sodium hypochlorite (NaOCl), lysozyme, and human β-defensin 3 (Table 1). The studies included antimicrobials which were either clinically appropriate (dental, NaOCl, (Halford, et al. 2012)), or were testing a new approach (lysozyme, (Liao, et al. 2017); human β-defensin 3, (Zhu, et al. 2013), (Li, et al. 2015), (Zhou, et al. 2018)). Sodium hypochlorite is a disinfectant used widely in endodontic irrigation and healthcare facilities (Estrela, et al. 2002). Human β-defensin 3, an endogenous broad-spectrum antimicrobial peptide produced by various cells in the human body (Dhople, et al. 2006), was either administered in free form or encapsulated in liposomes (Zhou, et al. 2018). The aim was to load the liposomes onto SonoVue® microbubbles, but proof thereof was not provided. Lysozyme is a naturally occurring antimicrobial protein and was used in five (non-sonobactericide) papers as the microbubble coating material (Cavalieri, et al. 2008, Cavalieri, et al. 2012, Zhou, et al. 2012, Cavalieri, et al. 2013, Mahalingam, et al. 2015).

All sonobactericide studies used an appropriate antibiotic targeting a specific microbe, according to therapeutic guidelines (Mandell, et al. 2000, Mermel, et al. 2009, Osmon, et al. 2012, Baddour, et al. 2015, Habib, et al. 2015, Lanjouw, et al. 2016), excluding two studies which could not be linked to guidelines due to nondisclosure of microbe information beyond species (Lin, et al. 2015) and no disease aim (Zhu, et al. 2013). Two examples of correct antibiotic and microbe pairings are Sugiyama et al. (2018), who aimed to treat severe gram-negative bacterial pneumonia and used an *E. coli* strain for which the Canadian guideline recommends gentamicin (Mandell, et al. 2000), and Lattwein et al. (2018) who aimed to treat infective endocarditis and used a methicillin-susceptible *S. aureus* isolate for which both the European (Habib, et al. 2015) and American (Baddour, et al. 2015) guidelines recommend oxacillin. Additionally, of the studies using an antibiotic, 2 out of 9 focusing on Gram+ bacteria used strains already resistant to first-line antibiotics. Many infections are not dominated by resistant microbes, and Gram− bacteria can have higher resistance profiles than Gram+ (Hu, et al. 2018). This choice could be influenced by media coverage, strain access, or geographical location. All articles using vancomycin and methicillin-resistant microbes originated from China, which has high levels of reported antimicrobial resistance (Hu, et al. 2018).

A few groups performed sonobactericide using non-antimicrobial therapeutics. One paper used recombinant tissue plasminogen activator (rt-PA), a clinically approved fibrinolytic agent, in combination with the antibiotic oxacillin (Lattwein, et al. 2018). Two articles investigated gene transfection of plasmid DNA into planktonic bacteria (Han, et al. 2005, Han, et al. 2007). The microbubble-mediated accumulation of bone marrow mesenchymal stem cells, which can suppress inflammation, was investigated as a treatment for chronic bacterial prostatitis (Yi, et al. 2016). Although the majority of sonobactericide studies paired their treatments with therapeutics, five (19%) focused directly on the mechanical and

biological effects resulting from ultrasound and microbubbles alone (Vollmer, et al. 1998, Nishikawa, et al. 2010, Tandiono, et al. 2012, Agarwal, et al. 2014, Goh, et al. 2015).

Many of the *in vitro* studies were performed in polystyrene tissue culture well-plates, ranging from 96- to 6-well plates, for both planktonic and biofilm studies (10 studies, 37%; Table 1). To the well-plates, Zhu, et al.(2013) added a 10 mm diameter titanium plate (1 mm thickness), Guo, et al. (2017) a 13 mm and Fu, et al.(2019) a 12 mm glass coverslip, and Nishikawa et al. (2010) a polystyrene disk (dimensions not provided). Two studies also cultured biofilm in a FluoroDish, a 35 mm dish containing a 23.5 mm glass window (He, et al. 2011, Hu, et al. 2018). The geometry of both these containers could result in the reflection of ultrasound at the bottom of the well and at the medium-air interface. As a result, constructive and deconstructive interference leading to standing waves could have occurred (Coakley, et al. 1989). Standing waves may also form within the body, especially in the presence of bone (O'reilly, et al. 2010). Microbubbles may aggregate at the nodes of a standing wave (Shi, et al. 2013). Increases in *in situ* acoustic pressure caused by constructive interference can cause unwanted bioeffects mediated by inertial cavitation (Azuma, et al. 2005, Deffieux and Konofagou 2010). The presence of standing waves produces acoustic field variations that are sensitive to changes in transducer position, excitation frequency, or temperature (Huber, et al. 2011). The acoustic intensity of the ultrasound field is proportional to the square of the pressure amplitude when the ultrasound wavelength is much smaller than the transducer aperture (Kleven, et al. 2019). Under the plane wave approximation, the acoustic pressure is related to the intensity as follows: $I = P^2/2\rho c$ where P is the peak acoustic pressure, ρ is the density, and c is the speed of sound (Kinsler, et al. 2000). For traveling waves, the intensity is a function of time, i.e. once the wave has passed a given spatial location, the intensity drops to zero. However, for standing waves, the peak intensity at a spatial location remains constant over time. Effects of standing wave formation during insonation of cells in different holders have previously been investigated in detail (Hensel, et al. 2011).

Measuring the *in situ* acoustic parameters is critical to understanding and correlating the treatment effects to specific outcomes, and to translate these to an *in vivo* setting (Ter Haar, et al. 2011). Only five sonobactericide studies reported calibrating the output *in situ* (Tandiono, et al. 2012, Goh, et al. 2015, Ronan, et al. 2016, Lattwein, et al. 2018, Horsley, et al. 2019). The lack of standardization of exposure set-ups makes it difficult to compare the results in the literature. Reporting spatial maps of the acoustic field *in situ* could help improve the reproducibility and interpretation of *in vitro* studies between groups (Ter Haar, et al. 2011).

In the well-plates and FluorDishes, cavitation nuclei were administered once for treatment times varying from 20 s to 10 min (see Table 1), with the exception of one study in which fresh microbubbles were administered every 4 h for 24 h (Lin, et al. 2015). It is unclear whether microbubbles were still present beyond a few minutes during insonification due to destruction or dissolution. For example, Mannaris and Averkiou (2012) showed that SonoVue® microbubbles, insonified *in vitro* for 20 ms at 1 MHz using 10 cycle pulses at a PRF of 100 Hz, were destroyed and/or dissolved after only a few pulses at 400 kPa acoustic pressure, while microbubbles were still present after all pulses at an acoustic pressure of

100 kPa. In addition, longer than 100 cycle pulses at acoustic pressures > 0.4 did not give any added benefit in terms of microbubble oscillation. One group used the OptiCell™ cell culture system for their biofilm experiments (Dong, et al. 2013, Dong, et al. 2017), which consists of two gas permeable, thin (75 μm) polystyrene membranes, spaced parallel and 2 mm apart providing 50 cm^2 area of cell culture. Microbubbles were administered once for a 5 min treatment (0.3 or 1 MHz, 0.12 MPa, 50% duty cycle) period.

Several groups used a less commercial *in vitro* set-up. Goh et al. (2015) used an acetate film square chamber with the top and right side consisting each of a coverslip and the ultrasound (250 kHz or 1 MHz, 0.1 – 1 MPa, 50 μs pulse) transducer positioned below. One cover slip had a biofilm, such that the microbubbles were either floating beneath the biofilm or optically trapped at varying distances from the side. Lattwein et al. (2018) performed sonobactericide under plasma flow (0.65 mL/min) on biofilms grown statically on human whole blood clots placed in glass capillaries (2.15 mm inner diameter). Microbubbles were continuously infused and ultrasound (120 kHz, 0.44MPa, continuous wave, 50 s on 30 s off) was applied intermittently for 30 minutes. Ronan et al. (2016) grew biofilms in a cylindrical flow cell (17 mL/h) with an acoustically transparent membrane on one side and a glass coverslip on the other, and flow was halted to perform sonobactericide (0.5 MHz, 1.1 MPa, 16 cycle tone burst, PRF 1 kHz) for 5 min, with microbubbles administered once. Flow was also used by Tandiono et al. (2012) to treat planktonic bacteria in a microfluidic system comprised of polydimethylsiloxane-made channels. In humans, biofilms can develop in variable fluid flow environments depending on the location, or under a static condition. Biofilms are highly sensitive to these different conditions (Thomen, et al. 2017). Thus selection of the appropriate static or flow condition setting should be tailored to the specific aimed application, such as superficial skin wound or intravascular device infections.

For dental application, Halford et al. (2012) grew biofilms in the root canal (12 mm length) of single-rooted extracted human teeth under constant agitation (120 rpm). Microbubbles were delivered into canals and insonified by a P5 Newtron dental ultrasonic hand piece (28–36 kHz ultrasound) for 1 min. Horsley et al. (2019) used a bladder organoid model using a modified acoustically compatible chamber (Carugo, et al. 2015). Briefly, a polycarbonate filter insert (12 mm diameter) cultured with infected human bladder cells was fixed between an Ibidi culture dish (35 mm) and a polydimethylsiloxane lid. Cavitation nuclei were added, the dish and lid were coupled, and then insonified (1.1 MHz, 2.5 MPa, 5500 cycles, 20 ms pulse duration) for 20 s. Other *in vitro* experimental set-ups were on nylon membranes (47 mm diameter, pore size of 0.2 μm) and in centrifuge tubes (2 and 5 mL) (Table 1). Nylon membrane biofilms were treated in a beaker placed in a sonicator (0.042 MHz, on for 2 s every 2 min) while microbubbles were continuously introduced for 15 minutes (Agarwal, et al. 2014). The planktonic bacteria in tubes were treated (1 MHz, 500 W/cm^2, 2% duty cycle) for 5 min (Vollmer, et al. 1998) or for 12 h (0.0465 MHz, 0.01 W/cm^2, 33% duty cycle) (Zhu, et al. 2014) and in eppendorf tubes (1 MHz, 1–3 W/cm^2, 50% duty cycle) for 1 min (Liao, et al. 2017), all with a one-time administration of microbubbles.

Three *in vitro* studies followed up with a corresponding *in vivo* study in the same article (He, et al. 2011, Lin, et al. 2015, Liao, et al. 2017). Thirty percent of sonobactericide articles (8/27) have investigated therapeutic efficacy in preclinical animal models (Table

1). Four groups chose to emulate implanted medical device infections using subcutaneous implants, near the spine, with biofilm grown on catheter pieces or polyethylene disks in rabbits (He, et al. 2011, Dong, et al. 2018) and titanium plates in mice (Li, et al. 2015, Zhou, et al. 2018). Microbubbles were injected subcutaneously into the implant area before ultrasound. For each of the three ultrasound exposures (20 min) per a day, He et al. (2011) injected 200 μl microbubbles (2×10^8 – 5×10^8/mL) every 5 min, and both Li et al. (2015) and Zhou et al. (2018) injected 30 μl once, 2×10^8 – 5×10^8/mL and concentration not disclosed, respectively. Dong et al. (2018) applied ultrasound twice a day for 5 min, and injected 500 μl (1.2×10^9/mL diluted to 1% (vol/vol)) each time. All studies used a 50% duty cycle. However acoustic parameters, treatment intervals, and duration times varied (Table 1).

Lin et al. (2015) investigated the ability of sonobactericide to increase the elution rate of antibiotics from vancomycin-loaded bone cement in a periprosthetic infection rabbit tibia model. Ultrasound (1 MHz, 0.3 W/cm^2, 30% duty cycle) was applied transcutaneously for 24 h and microbubbles (2×10^8 – 5×10^8/mL) were injected into the same space as the *S. aureus* bacteria at four time points. Surrounding tissues were evaluated directly following treatment. For chronic bacterial prostatitis modeled in rats, Yi et al. (2016) used sonobactericide to induce accumulation of bone marrow mesenchymal stem cells to reduce inflammatory reactions and resolve infection. After four weeks of infection induction with *E. coli*, microbubbles (0.1 mL/kg) were directly injected into prostates and insonified (1 MHz, 0.5 MPa, 1% duty cycle) for 5 min. Afterwards, stems cells (1×10^7) were administered intravenously and therapeutic effectiveness was evaluated after 24 h and 2 wk.

Another study focused on harnessing sonobactericide in a model of severe bacterial pneumonia with the goal of enhancing antibiotic delivery to infected lung tissue in mice (Sugiyama, et al. 2018). *E. coli* were administered intratracheally and six hours later gentamicin was injected intraperitoneally. After thirty minutes, microbubbles (1×10^9) were intravenously administered and ultrasound (1.3 MHz, 0.9–1.2 MPa, pulse every 5 s; pulse duration not specified) transmitted thoracically for 5 min. Lavage and tissues samples were evaluated at 30 min and 2 h, respectively, after ultrasound application. Liao et al. (2017) also used mice and aimed to improve acne vulgaris treatment using transdermal sonobactericide with lysozyme-shelled microbubbles. Ears were infected intradermally with *Propionibacterium acnes*. Gel loaded with lysozyme microbubbles was placed on top of the infected area and insonified (1 MHz, 3 W/cm^2, 50% duty cycle) every day for 1 min. Effectiveness was assessed at several time points during the 13 d of treatment.

Various techniques were used for assessing sonobactericide efficacy. The colony-forming units (CFU) plate-counting method was utilized to determine antimicrobial efficacy (14/27, 52%), for some *in vitro* and all *in vivo* studies except one (Yi, et al. 2016). Bacterial plating is relatively easy to perform and considered the “gold standard” for determining viable bacteria counts. This technique, however, is widely known to underestimate the absolute number of bacteria. Another potential limitation is that often to obtain post-treatment samples, biofilms have been mechanically disrupted, scraped, centrifuged, digested, vortexed, or sonicated, which might have induced microbial alterations. Several papers employed histopathologic staining, either crystal violet or hematoxylin and eosin, for observing bacterial morphology (macroscopy and light microscopy), quantifying biofilm

density by absorbance levels in a microplate reader, or comparing inflammatory effects over time. This method can be used for high throughput screening, but it does not discriminate between live and dead cells. Immunohistochemistry was used by Yi et al. (2016) to quantify inflammatory cytokine expression and distribution. Agarwal et al. (2014) desiccated their mixed species biofilms to determine fixed biomass for overall density quantification, and also, albeit with additional steps, for extracellular protein and polysaccharide content.

Several microscopic techniques were utilized for visualization of treatment, including light, epifluorescence, confocal laser scanning, transmission and scanning electron microscopy. Light microscopy was combined with or without time-lapse and high-speed camera observations (Halford, et al. 2012, Tandiono, et al. 2012, Goh, et al. 2015, Lattwein, et al. 2018); see Figure 3 for a light microscopy example. Fluorescence detection, either with a widefield or confocal microscope, was the most utilized optical imaging modality to qualitatively and quantitatively visualize live and fixed-cell populations (16/27, 59%). These images can provide information not only on the viability status, but also biomass, average biofilm thickness, and structural heterogeneity. Live/dead nucleic acid staining with Syto 9 (viable cells) and propidium iodide (dead or membrane-disrupted cells) were often used and observed with confocal microscopy (Figure 4) to assess biofilm populations. Note that biofilm nucleic acid fluorescent signals might not only indicate single bacterium, but also extracellular DNA found throughout many biofilms (Okshevsky and Meyer 2014). For investigating biofilm compositional changes, extracellular proteins were stained with fluorescein isothiocyanate (FITC), lipids with Nile red, and α- and β-polysaccharides with lectin concanavalin A conjugated with tetramethyl rhodamine and fluorescent brightener, respectively (Agarwal, et al. 2014). These polysaccharides (α, β) can also be visualized with FITC-conjugated lectin concanavalin A and wheat germ agglutinin (Anastasiadis, et al. 2014). Scanning and transmission electron microscopy were used for post-treatment ultrastructural observations of planktonic bacteria and biofilm morphology (10/27; 37%). Scanning electron microscopy (Figure 5) was also used to complement confocal findings (Dong, et al. 2013, Zhu, et al. 2013, Li, et al. 2015, Guo, et al. 2017, Dong, et al. 2018, Zhou, et al. 2018). For transmission microscopy, sample preparation of biofilms required removal from culture plate and thus were mechanically scraped, which could alter cellular structure (Hu, et al. 2018).

Genetic testing was performed in seven studies, using the polymerase chain reaction (PCR) method (Han, et al. 2005, Han, et al. 2007, Tandiono, et al. 2012, Zhu, et al. 2013, Li, et al. 2015, Yi, et al. 2016, Dong, et al. 2017, Zhou, et al. 2018). PCR was used to investigate the impact of sonobactericide on the expression of genes (Zhu, et al. 2013, Li, et al. 2015, Dong, et al. 2017, Zhou, et al. 2018) and mRNA (Yi, et al. 2016), the successful incorporation of a gene (Han, et al. 2005, Han, et al. 2007) and the status of genes up- and downstream after incorporation (Han, et al. 2005), and to quantify intracellular DNA released into the supernatant after treatment, which provided an indication of disrupted (lysed) cells (Tandiono, et al. 2012). As advantages, PCR techniques are not technically demanding, fast, and highly sensitive. High sensitivity is also a disadvantage concerning contamination, along with the specific target of interest must already be known, and caution should be taken in interpreting the results due to the potential for extracellular DNA released from bacteria not triggered by lysis. Two studies, investigating intracellularly infected mammalian

cells, evaluated cytotoxicity in response to therapy using either a trypan blue exclusion test (Ikeda-Dantsuji, et al. 2011) or a lactate dehydrogenase assay (Horsley, et al. 2019).

Changes in biofilm metabolism, in response to different treatments, were measured by confocal imaging with 5-Cyano-2,3-ditolyl tetrazolium chloride dye (Hu, et al. 2018), a CO_2-evolution monitoring system (Ronan, et al. 2016), or an absorbance-based resazurin assay (Guo, et al. 2017, Fu, et al. 2019). While investigating cellular metabolism provides an indication of the overall bioeffect, the growth rate, biomass, cell viability, or persistor development could not be specified. Vollmer et al. (1998) and Yi et al. (2016) used bioluminescence as an indicator of bacterial cell stress-responses and the distribution of stem cells in rats, respectively. Besides using fluorophore internalization, one group used a fluorescence polarization immunoassay to determine the amount of vancomycin eluted from bone cement following *in vitro* treatments (Lin, et al. 2015). An enzyme-linked immunosorbent assay was also used after treatments to determine levels of gentamicin (Sugiyama, et al. 2018) and inflammatory cytokines (Yi, et al. 2016) in tissue. Both immunoassays are highly specific, even in samples with protein content such as serum (Yu, et al. 2010, Odekerken, et al. 2015), and are commercially available for various antibiotics on the market.

CAVITATION NUCLEI FOR SONOBACTERICIDE

Cavitation nuclei are a key part of sonobactericide because their volumetric changes in response to an ultrasound field induce bioeffects. From the commercially available cavitation nuclei, SonoVue® was used most (eight studies, 30%). SonoVue® (available as Lumason® in the USA (Lumason® 2016)) consists of SF_6 gas microbubbles (mean diameter 1.5–2.5 μm; ≥ 99% of microbubbles ≤ 10 μm) stabilized by a lipid coating (Schneider, et al. 1995). SonoVue®/Lumason® is approved for clinical diagnostic use in several countries worldwide (Nolsoe and Lorentzen 2016). Other commercially available lipid-coated microbubbles have also been used for sonobactericide studies, namely Definity® (four studies, 15%, (octafluoropropane (C_3F_8) gas core; mean diameter 1.1–3.3 μm; 98% of microbubbles < 10 μm) (Definity® 2011) and Sonazoid® (1 study, 4%, C_4F_{10} gas core; mean diameter 2.1 μm± 0.1; < 0.1% of microbubbles larger than 7 μm) (Sontum 2008). Definity® and Sonazoid® are approved for clinical diagnostic use in several countries worldwide (Nolsoe and Lorentzen 2016). Note that Albunex®, used by Vollmer et al. (1998), was the first commercially available ultrasound contrast agent (in 1992), with a mean microbubble diameter of 3.8 μm (98.8% of microbubbles < 10 μm), an air core, and a human albumin coating (Feinstein 1989). However, Albunex® is no longer available (Mayer and Grayburn 2001). Optison™ is another human albumin coated microbubble (C_3F_8 gas core; mean diameter 3.0–4.5 μm; 95% of microbubbles < 10 μm (Optisontm 2012)) and approved for clinical use in the United States and Europe. Vollmer et al. (1998) also used custom-made microbubbles (ST68; mean diameter 3.8 μm; air core; coating mixture of surfactants, Span 60 and Tween 80 (Forsberg, et al. 1997)) in their study.

The advantage of using commercially available cavitation nuclei is that their response to ultrasound has been thoroughly characterized (Gorce, et al. 2000, Moran, et al. 2002, Chen, et al. 2003, Chetty, et al. 2008, Guidi, et al. 2010, Faez, et al. 2011, Helfield and Goertz

2013). In addition, these cavitation nuclei are sterile with minimal batch-to-batch variability. On the other hand, custom-made cavitation nuclei as used in eleven of the sonobactericide studies can offer advantages, such as targeting by incorporating a ligand in the coating and drug loading.

While several types of targeted microbubbles exist for ultrasound molecular imaging and drug-loaded microbubbles for ultrasound-mediated drug delivery, or a combination thereof (Sutton, et al. 2013, Kooiman, et al. 2014, Van Rooij, et al. 2015), so far only one study has employed targeted microbubbles to *S. aureus* biofilms *in vitro* using a monoclonal immunoglobulin antibody to protein A or a lectin from *P. aeruginosa* for ultrasound molecular imaging (Anastasiadis, et al. 2014). These targeted microbubbles were found to bind to the biofilm matrix in proportion to the surface area.

A few studies have reported on drug-loaded microbubbles or droplets for treatment of bacterial biofilms. Horsley et al. (2019) conjugated custom made gentamicin-loaded liposomes onto microbubbles (ratio 1:5) using biotin-avidin bridging (mean diameter 5.79 μm ± 1.53 μm). The microbubbles had a gas core of SF_6 and the lipid coating consisted of 1,2-distearoyl-sn-glycero-3-phosphocholine (DSPC), 1,2-distearoyl-sn-glycero-3-phosphoethanolamine-N-carboxy (poly-ethyleneglycol) (DSPE-PEG(2000)), DSPE-PEG-biotin, and 1,2-dipalmitoylsn-glycero-3-phosphoethanolamine-N-(lissamine rhodamine B sulfonyl)(ammonium salt) (Rod-PE) in a molar ratio of 79.5:10:10:0.5. The protein lysozyme was used as drug and also formed the coating of microbubbles. One study custom made these microbubbles with an air gas core (mean diameter of 4 ± 1 μm or 6 ± 2 μm, depending on the duration of protein denaturation; 15 minutes and 2 minutes, respectively) (Cavalieri, et al. 2008, Zhou, et al. 2012), and another used C_3F_8 (mean diameter 2.5–2.9 μm, depending on the sonication power) (Liao, et al. 2017). Lysozyme-coated microbubbles loaded with either spherical bovine-serum-albumin-coated gold nanoparticles (4.5 nm diameter) or polyvinylpirrolidone-coated gold nanoparticles (15 nm diameter) were also produced by Cavalieri et al. (2013). Both types of gold nanoparticles had no effect on the microbubble size distribution or stability. Mahalingam et al. (2015) produced poly(vinyl alcohol)-lysozyme-coated microbubbles (10–250 μm; nitrogen gas core) loaded with gold nanoparticles (average diameter ~10 nm). These microbubbles were more stable when they contained the gold-nanoparticles than without them, which is in in contrast to what Cavalieri et al. (2013) found. The difference in the type of coating or microbubble size could be the reason for the difference in stability.

Nanodroplets that can be phase-transitioned into microbubbles using ultrasound, a phenomenon known as acoustic droplet vaporization (Kripfgans, et al. 2000, Lin and Pitt 2013), have been loaded with the antibiotic vancomycin by Argenziano et al. (2017). The nanodroplets (average diameter ~300 nm) had a core of perfluoropentane and shell of lipid and dextran sulfate to which the vancomycin was coupled by electrostatic interaction. The authors sterilized their formulation using ultraviolet light. The nanodroplets (mean diameter 309 nm) made by Guo et al. (2017) consisted of a core of perfluoropentane and a coating of lipids. Microbubbles (mean diameter 1.5 μm) containing a C_3F_8 gas core and coating of the same lipids were also produced.

Four groups produced custom microbubbles for co-administration studies with an antibiotic (Ikeda-Dantsuji, et al. 2011, Dong, et al. 2013, Dong, et al. 2017, Dong, et al. 2018), an antibiotic encapsulated in a liposome (Fu, et al. 2019), or stem cells (Yi, et al. 2016). Dong et al. produced lipid-coated microbubbles with a gas core of C_3F_8 with a diameter of 4 – 6 μm (Dong, et al. 2013, Dong, et al. 2017, Dong, et al. 2018). The coating consisted of the lipids DSPC and 1,2-dipalmitoyl-sn-glycerol-3-phosphor-ethanolamine (DPPE), molar ratio 66:34. The microbubbles were sterilized by ^{60}Co irradiation. Ikeda-Dantsuji et al. (2011) produced microbubbles (~1 μm) encapsulating C_3F_8 gas with a lipid coating of DSPC and DSPE-PEG(2000), molar ratio 94:6. Microbubbles (mean diameter 2.39±0.05 μm) with a coating of 1,2-dipalmitoyl-sn-glycero-3-phosphocholine (DPPC), DSPE, and cholesterol, mass ratio of 10:4:1, and a C_3F_8 gas core were produced by Fu et al.(2019). A thorough characterization of the response of these microbubbles to ultrasound was not reported in these publications. The lipid-coated microbubbles (1,2-dipalmitoyl-sn-glycero-3-phosphoglycerol (DPPG), DSPC, and PEG4000 with mass ratio 30:30:3000 (W:W)) with a C_3F_8 gas core (mean 2 μm) by Yi et al. (2016) were compared to SonoVue® for liver imaging (Liu, et al. 2011). Enhancement was similar but persisted longer (still present 6 min 30 s after injection) for these custom-made microbubbles.

In the study by Halford et al. (2012), microbubbles were produced during ultrasound treatment (28–36 kHz) from a solution containing perfluorodecahydronaphthalene as oxygen carrier, 30% hydrogen peroxide, or H_2O_2, as oxidizer, and the non-ionic detergent surfactant Triton-X100 as shell stabilizer. The figure of the formed microbubbles indicates microbubble diameters on the order of 200 μm. Non-coated microbubbles were also produced during ultrasound treatment (130 kHz) in the study by Tandiono et al. (2012). In another study, non-coated microbubbles with a mean size of 5–10 μm were produced with a microbubble generator (Agarwal, et al. 2014). No specifics on the gas core and microbubble coating were provided.

The synergy between microbubbles and ultrasound exposure parameters is important for sonobactericide because the radial pulsation of microbubbles may increase the “footprint” of bactericidal action and reduce treatment times. The oscillation of each microbubble highly depends on its resonance behavior, i.e. the ultrasound frequency at which the amplitude of oscillation is largest. In general, the resonance frequency is inversely related to the microbubble diameter, but the properties of the microbubble coating also play a role as rigid microbubble coatings increase the resonance frequency (Leighton 1994, Kooiman, et al. 2014). Interestingly, 78% (21/27) of sonobactericide studies used lipid-coated microbubbles, see Table 1. A small fraction of the commercially available microbubbles is resonant for a particular insonification scheme, because of the polydisperse population (Hettiarachchi, et al. 2007). Different ultrasound center frequencies were used for sonobactericide, including frequencies used in clinical diagnostic imaging (1 MHz (13 studies) and 1.3 MHz (1 study), see Table 1). At these frequencies, only a sub-population of the microbubbles are expected to oscillate in resonant modes. The ultrasound frequency employed in the other studies was lower, namely 500 kHz (1 study), on the order of 300 kHz (4 studies), 120–130 kHz (2 studies), or between 28 and 80 kHz (7 studies). For these very low ultrasound frequencies, only microbubbles substantially larger than 10 μm in diameter would have been at resonance. Gas from the microbubbles was likely liberated, coalesced, and grew

by rectified diffusion in the acoustic field until the microbubbles reached resonant size (Postema, et al. 2002, Bader, et al. 2015). Another important consideration for microbubble oscillation is the viscosity of the surrounding medium and confinement because oscillations are damped when the viscosity increases or when microbubbles are confined (Kooiman, et al. 2014). For the *in vivo* studies, the microbubbles were confined in tissue due to injection into the area of the implanted catheter (Dong, et al. 2018), dish (He, et al. 2011), titanium plate (Li, et al. 2015), or tibial canal (Lin, et al. 2015). It appears that these studies did not consider the effect of attenuation of ultrasound by overlying tissue.

EXPERIMENTAL OUTCOMES

All sonobactericide studies have demonstrated an enhanced effect beyond that of antibiotics alone. The goal of all of these studies was proof-of-principle and generally approached differently. Directly comparing these twenty-seven articles is difficult because of the large variability that exists between them. Differences between the groups include the bacteria used, the different growth conditions, ultrasound parameters, cavitation nuclei, and experimental set-ups. Nevertheless, this section aims to provide discussion and make general comparisons between the experimental outcomes.

Ultrasound interacts with tissue by heating (Haar 2010), radiation force (Nyborg 1953), and cavitation-based mechanisms (Dalecki 2004, Ter Haar 2009). Heating and radiation force could enhance the effect of antibiotics (Hajdu, et al. 2010) increasing membrane permeability (Juffermans, et al. 2006) and cell detachment, respectively. Cavitation is an important mechanism for sonobactericide. Stable cavitation involves gentle oscillations of microbubbles (Bader and Holland 2013), and inertial cavitation denotes the rapid growth and rapid collapse of microbubbles (Holland and Apfel 1989). The acoustic pressure required to initiate inertial cavitation can be higher than the pressure required for stable cavitation (Bader and Holland 2013) and also depends on fluid properties and the cavitation nuclei (Apfel 1997). Inertial cavitation forms microjets (Ohl, et al. 2015) that can damage or deform the biofilms (Goh, et al. 2015). Administration of cavitation nuclei can reduce the cavitation threshold (Bader and Holland 2013).

When microbubbles oscillate in an ultrasound field, fluid flow is generated around the microbubbles (Elder 1959, Leighton 1994). This phenomenon is known as microstreaming. The effects of microstreaming are prominent when the oscillating bubble is located near a boundary, and when it is excited at resonance (Leighton 1994). Microstreaming can cause bioeffects by promoting fluid transport and producing shear stresses on cells (Collis, et al. 2010). Microbubble destruction in response to ultrasound can happen through either acoustically driven diffusion or through microbubble fragmentation (Chomas, et al. 2001). Fragmentation in response to ultrasound exposure is typically associated with inertial cavitation (Shi, et al. 2000) and can produce mechanical bioeffects.

Table 1 shows that the majority of sonobactericide studies used one pressure amplitude, or acoustic intensity, and one center ultrasound frequency. Four studies tested multiple pressures/intensities (Han, et al. 2007, Ikeda-Dantsuji, et al. 2011, Goh, et al. 2015, Liao, et al. 2017) and one employed two frequencies (Goh, et al. 2015). Ikeda-Dantsuji et al.

(2011) demonstrated that a higher ultrasound intensity (0.44 W/cm^2) further increased sonobactericide efficacy above doxycycline alone by approximately three times that of the lower intensity setting (0.15 W/cm^2). However, when another antibiotic (ceftizoxime), to which *Chlamydia trachomatis* is resistant, was employed they found that the higher ultrasound intensity only slightly improved the therapeutic efficacy further. Liao et al. (2017) found that higher intensity insonification (2 and 3 W/cm^2) beyond 1 W/cm^2 did not further enhance sonobactericide. Han et al. (2007) also found that as the acoustic pressure increased (0.25, 0.5, >0.9 MPa), delivery of their model drug into bacteria correspondingly increased.

Other ultrasound parameters were explored, such as pulse repetition frequency (0–100 Hz), duty cycle (5 and 50%), concentration of cavitation nuclei (0, 3.3, 10, 33% vol/vol), and exposure duration (0, 10, 90, 450 s) (Han, et al. 2007). An increase in efficacy was seen with corresponding increased parameters, except pulse repetition frequency which had no increased effect. As desired, bacteria viability was not affected among the parameters tested by Han et al. (2007) for the creation of a recA positive strain of *Fusobacterium nucleatum*. RecA renders bacteria more sensitive to ultraviolet light and reportedly repairable sonoporation (Han, et al. 2007). Using similar sonobactericide conditions also on planktonic, exponential growth phase, Gram− bacteria, albeit with *E.coli*, Vollmer et al. (1998) found bacterial death (up to 49.7 ± 6.2%) and activation of stress-response genes.

Goh et al. (2015) used high-speed optical imaging to investigate the impact of cavitating microbubbles on biofilm surfaces. At 0.1 MPa (1 MHz, 50 μs pulse), microbubble oscillation was reported to be small, and caused minimal biofilm disruption. At a higher pressure (0.7 MPa; 1 MHz; 50 μs pulse)), a 7.4 μm SonoVue® microbubble had an extremely large radial excursion (R_{max} 27.3 μm) with a liquid jet within that led to bacteria being mechanically dislodged from the biofilm. The direction of a jet with respect to the surface of the biofilm depends on the elasticity of the surface (Ohl, et al. 2015). Accordingly, jet formation can create substantial shear force leading to either an indentation or invagination of the surface (Chen, et al. 2011, Chen, et al. 2012). Although Goh et al. (2015) used two ultrasound frequencies (0.25 and 1 MHz), they applied each frequency in a different set-up (biofilm horizontally or vertically positioned). Therefore, the effects due to different frequencies could not be compared. They found that ultrasound parameters and the distance between the biofilm surface and the cavitating microbubbles affected the efficacy of biofilm disruption. Ultrasound alone did not disrupt the biofilm structure. As the initial distance between the microbubble and the biofilm increased, the disruption efficacy decreased. This observation provides support for the use of biofilm-targeted microbubbles to increase the efficacy of sonobactericide.

Ronan et al. (2016) also described biofilm disruption, in the form of craters, following ultrasound and microbubbles exposure without antibiotics (Figure 4). If bacteria are forcibly released from biofilms due to microbubble oscillations, as suggested by several studies including Ronan et al. (2016) and Goh et al. (2015), then the viability and status of these dispersed cells following treatment need to be assessed. Sonobactericide could be combined with current “traditional” or other new antimicrobials, for reducing the spread of or eliminating altogether transitional dispersed cells that may be more virulent. Planktonic bacteria are often sensitive to antibiotics at much lower concentrations than the same

bacteria in biofilms (Olson, et al. 2002). Thus liberation of bacteria into the bloodstream after sonobactericide is not anticipated to pose additional risks.

Inertial cavitation caused by ultrasound-mediated microbubble destruction can produce defects in the biofilm matrix, aiding the penetration of antibiotics (He, et al. 2011). Microbubbles and ultrasound exposure have been reported to increase the elution of an antibiotic from polymethylmethacrylate cement and increase efficacy of bactericidal treatment *in vitro* and *in vivo* (Lin, et al. 2015). Ultrasound-mediated microbubble destruction can also increase the metabolic activity of the bacteria in the biofilm, making it responsive to treatment with antibiotics (Hu, et al. 2018). However, Ronan et al. (2016) demonstrated a decreased biofilm metabolism, by analyzing carbon dioxide production, following either antibiotic alone or combined with ultrasound and microbubbles. Due to the experimental set-up, it could not be definitively determined if the decrease was from growth rate or biofilm mass reduction, and is speculated to be both. Although bacteria can develop resistance to antimicrobials over time by genetic alterations, ultrasound acts without allowing these organisms to adapt to the physical stresses (Vollmer, et al. 1998). Additionally, Zhou et al. (2018) found *in vivo* that the expression of the MecA gene responsible for encoding resistance to β-lactam antibiotics in MRSA was significantly lowered in the sonobactericide group with human β-defensin 3, and more than twice that of the antimicrobial alone.

It has been postulated that bacterial cells could be more susceptible to sonobactericide because of their rigid cell membranes, which contrasts with the compliant phospholipid bilayers of mammalian cells that may resist rupture due to ultrasound exposure (Conner-Kerr, et al. 2010). When ultrasound is combined with cavitation nuclei and an antibiotic, sonobactericide efficacy can be enhanced as demonstrated by the *in vitro* and *in vivo* studies in this review. For example, *in vitro* studies reported by Dong et al. (2013), utilized Sonovue® and reduced colony-forming units of *S. epidermidis* 8-fold relative to treatment with vancomycin and ultrasound (1 MHz frequency, 0.5 W/cm^2 intensity, 50% duty cycle, 5 min). In *in vivo* studies, findings of enhanced bacterial killing when sonobactericide included an antimicrobial were also reported, such as Sugiyama et al. (2018) with an almost 1-log reduction in colony-forming units compared to all controls. Sonobactericide could produce equivalent therapeutic effects at a lower antibiotic dose, which may reduce complications associated with systemic toxicity, especially with renal and liver complications. Sonobactericide may increase antibiotic (and other therapeutics) cytotoxicity; Horsley et al. (2019) reported higher toxicity in human urothelial cells with ultrasound exposed solutions of microbubbles coated with liposomes containing gentamicin at concentrations (2.64 and 5.28 μg/mL) than free gentamicin at the much higher clinically approved dosage (200 μg/mL). This finding highlights that cytotoxicity should be more widely considered as a sonobactericide test parameter in future studies.

Besides Han et al. (2007), the microbubble dose dependence of sonobactericide has been investigated by three other groups and found an increase in the efficacy of sonobactericide with increasing concentration of microbubbles (Ikeda-Dantsuji, et al. 2011, Dong, et al. 2013, Dong, et al. 2017), indicating dose dependent synergy. Only Han et al. (2007) used more than two concentrations, of which a near linear trend between microbubble

concentration and treatment efficacy could be observed. A similar increase in bioeffects with increasing microbubble concentration has been reported for sonoporation of eukaryotic cells (Ward, et al. 2000), and blood brain barrier disruption (Song, et al. 2017). Increasing the antibiotic concentration also resulted in a dose-effect increasing relationship for all treatments of *A. baumannii*, including both microbubbles combined with free polymyxin B and microbubbles with free chitosan-modified polymyxin B-loaded liposomes (Fu, et al. 2019). Horsley et al. (2019) increased both antibiotic and microbubble concentration, because gentamicin was encapsulated on liposomes bound to the microbubbles, which led to an enhanced reduction of bacterial load in infected urothelial cells.

The "in vial" concentration of Definity® is 4.2×10^9 microbubbles/ml, of Albunex® is 7×10^8 microbubbles/mL (Christiansen, et al. 1994), and of SonoVue®/Lumason® 3.0×10^8 to 1.1×10^9 microbubbles/mL. Assuming a blood volume of 5 L in an average human, the *in vivo* concentrations for Definity®, Albunex®, and Lumason® correspond to 8.4×10^5/mL, 1.4×10^5/mL, and 6×10^4/to 2.2×10^5/mL, respectively. Several sonobactericide studies reported thus far have used high concentrations of microbubbles (10^7 to 10^8/mL) both *in vitro* (Vollmer, et al. 1998, Dong, et al. 2013, Dong, et al. 2017, Hu, et al. 2018) and *in vivo* (He, et al. 2011, Li, et al. 2015, Dong, et al. 2018), relative to the concentrations currently used in clinical diagnostic imaging. This approach could potentially be employed in non-vascular applications such as dental biofilms, or implant biofilms (He, et al. 2011, Li, et al. 2015, Dong, et al. 2018). Furthermore, preclinical studies in both small animal and rodent models suggest that high concentrations of microbubbles administered intravenously, up to 250 times higher than the clinical dose, may be well tolerated (Schneider, et al. 2011). Although *in vitro* studies have shown that large microbubbles (~ 0.3 mm) can destroy biofilms under flow by microbubble collision (Sharma, et al. 2005, Parini and Pitt 2006), this mechanism is unlikely to occur for microbubbles of clinically relevant sizes for vascular applications (i.e. 1–10 μm).

Five studies used custom-made lysozyme-coated microbubbles in the absence of ultrasound (Cavalieri, et al. 2008, Cavalieri, et al. 2012, Zhou, et al. 2012, Cavalieri, et al. 2013, Mahalingam, et al. 2015). These showed antimicrobial properties on *Micrococcus lysodeikticus*, *S. aureus*, and *E. coli.* Lysozyme-coated microbubbles, or poly(vinyl alcohol)-lysozyme-coated microbubbles, loaded with gold nanoparticles were found to have a stronger antimicrobial effect than non-loaded microbubbles on planktonic *M. lysodeikticus* (Cavalieri, et al. 2013) and *E. coli* (Mahalingam, et al. 2015). The coated gold nanoparticles alone lacked lytic activity in the Cavalieri study, and thus the authors attributed the enhanced antimicrobial effect of the gold-nanoparticles loaded on the lysozyme-microbubbles to improved binding and consequently increased interaction of the bacteria with the surface of the lysozyme-microbubbles. Contrarily, gold nanoparticles alone produced an antibacterial rate of ~50% at 3 h in the Mahalingam et al. (2015) study. The difference in antibacterial activity of gold nanoparticles could be explained by the different bacteria employed. Combining these lysozyme-coated microbubbles with ultrasound could have further enhanced the antimicrobial properties as Liao et al. (2017) observed when using them in their *in vitro* and *in vivo* study. Sonobactericide used against *P. acnes* had an enhanced antibacterial effect and resulted in a 1.45-fold reduction in inflammatory reactions relative to

lysozyme-coated microbubbles alone. Furthermore, after 13 days of treatment, inflammation was no longer observed.

Vancomycin-loaded nanodroplets (Argenziano, et al. 2017), in the absence of ultrasound, were significantly more effective at an earlier time point than vancomycin alone or non-loaded nanodroplets alone in killing planktonic MRSA (isolated from human ulcerated wounds). The authors attributed their findings to the time-sustained release of vancomycin from the loaded nanodroplets. However, the altered charge could also have played a role since vancomycin is positively-charged and the vancomycin-loaded nanodroplets are negatively-charged. Ultrasound exposure significantly enhanced vancomycin delivery from the loaded nanodroplets *ex vivo* through non-infected porcine skin showing potential to treat skin infections (Argenziano, et al. 2017).

CLINICAL TRANSLATION OF SONOBACTERICIDE

Diagnostic ultrasound contrast examinations are performed worldwide (Madsen and Rasmussen 2011, Wei 2012, Alzaraa, et al. 2013, Nolsoe and Lorentzen 2016), including for the detection of the metastatic spread of bacterial infective endocarditis (Menozzi, et al. 2013a, Menozzi, et al. 2013bSSubmitting). Fifteen out of the 27 sonobactericide studies (56%) used microbubbles that are clinically approved, such as by the United States Food and Drug Administration and European Medicines Agency, which could help with the translation of sonobactericide into the clinic. Contrarily, sonobactericide with custom-made microbubbles containing Triton (Halford, et al. 2012) is not translatable because this surfactant is toxic to cells (Jahan, et al. 2008, Koley and Bard 2010).
The ideal characteristics of a clinically-relevant treatment can be broadly described as one that leads to improved patient outcomes, reduction in treatment times, and practical implementation in the clinic. More specifically, broad-spectrum bactericidal activity, low risk for inducing resistance, and minimal mammalian cell cytotoxicity could be considered. The reader is referred to two review articles that provide conceptional discussions on the ideal antibiotic that could aid sonobactericide strategies (Lewis 2013, Gajdács 2019). The use of clinically relevant animal models of biofilm would help translate the development of sonobactericide. For example, Lin et al. (2015) used a periprosthetic infection rabbit tibia model. However, periprosthetic joint infection models have limited translational value as described in the review by Carli et al. (2016). While proposing criteria for an optimal animal model, this review stresses the critical importance of animal, pathogen, implant, and outcome measurement selection, and a method that replicates the “human” periprosthetic environment, where in at least one of these areas current models fall short.

The choice of ultrasound insonification parameters is important for the clinical translation of sonobactericide. A wide frequency range (tens of kHz to 1.3 MHz) has been reported for sonobactericide, see Table 1, along with pulsed (Vollmer, et al. 1998, Lin, et al. 2015, Horsley, et al. 2019), continuous wave (Zhu, et al. 2013, Fu, et al. 2019), or intermittent ultrasound insonification (Agarwal, et al. 2014, Lattwein, et al. 2018). More studies directly investigating different ultrasound parameters should be performed to better understand the effect they have on sonobactericide. The choice of frequency and exposure parameters needs to focus on safety, efficacy, and compatibility with existing clinical workflows for

rapid clinical translation. Several *in vitro* studies have been conducted in sonication baths at frequencies ranging from 20 – 80 kHz (Zhu, et al. 2013, Zhu, et al. 2014), which are likely not directly suitable for *in vivo* applications. Physiotherapy probes (He, et al. 2011, Li, et al. 2015, Hu, et al. 2018) and gene transfer equipment (Dong, et al. 2013, Dong, et al. 2017, Hu, et al. 2018, Fu, et al. 2019) have also been adapted for sonobactericide studies. Development of specialized probes may be necessary for treating biofilms that are not easily accessible or where a small geometric footprint may be needed. Ultrasonic energy may be delivered to infected areas either extracorporeally, or using catheter-based ultrasound probes. Catheters have been reported previously for sonothrombolysis (Owens 2008, Kim, et al. 2017), and could be investigated for sonobactericide in vascular organs.

The microbubble concentration, type, and route depend on the location of the biofilm being treated. Microbubbles can be delivered intravenously, intraarterially, or by direct injection to the site of interest (Goldberg, et al. 1994). When necessary, high concentrations can be achieved site-specifically by local infusion of microbubbles. On the other hand, delivering microbubbles to biofilm infections associated with prosthetic joints may be challenging because the biofilm is typically located within the joint space (Mcconoughey, et al. 2014). In the case of bacterial infective endocarditis, contact between the microbubbles and the biofilm may be hampered by rapid pulsatile blood flow. Targeting the microbubbles to the biofilm could further aid in therapeutic efficacy. Clinical phase 0 trials have successfully been completed for ultrasound molecular imaging of prostate, ovarian, and breast cancer using targeted microbubbles (Smeenge, et al. 2017, Willmann, et al. 2017), thereby paving the way for clinical use of targeted microbubbles. The *S. aureus* biofilm-targeted microbubbles developed by (Anastasiadis, et al. 2014) lack clinical translation because the *P. aeruginosa* lectin used as ligand causes red blood cell agglutination (Gilboa-Garber and Sudakevitz 1999) and the protein A antibody used as ligand must compete with host antibodies that cover protein A (Bröker, et al. 2014). For other potential targeting possibilities, the reader is referred to the reviews by van Oosten et al. (2015) and Koo et al. (2017).

CONCLUSIONS AND FUTURE PERSPECTIVES

Therapeutic effects of sonobactericide can include direct bacterial killing, biofilm degradation and dispersal, and increased or synergistic therapeutic effectiveness of antimicrobials or other drugs, all resulting from the physical phenomena of ultrasound combined with cavitation nuclei aided by the addition of an antimicrobial agent. It is the different time scales at which these actions occur that makes sonobactericide challenging, as illustrated in Figure 6. The time scale of the microbubble vibration is on the order of microseconds in a MHz ultrasound field, which is many orders of magnitude smaller than the time scale of physiological effects (ms), let alone that of biological effects (s – min) and clinical relevance (days to months). The link between, and the mechanistic aspects of, cavitation nucleation, the effect on (intracellular) bacteria/biofilms, and antimicrobial drug release and uptake needs to be elucidated in future studies to efficiently treat bacterial infections.

The effect of the biofilm type on sonobactericide efficacy has received limited attention. For example, the age and composition of the biofilm (Shen, et al. 2010) may contribute to its resilience to sonobactericide. The antibiotic penetration through biofilm decreases appreciably with the age of the biofilm (Carmen, et al. 2004). Additionally, biofilms formed *in vivo* may differ in composition and morphology to *in vitro* biofilm models (Bjarnsholt, et al. 2013). For example, recent research has shown that infective endocarditis can be a polymicrobial infection (Oberbach, et al. 2017). These effects should be elucidated in future preclinical and clinical studies, as also addressed in other reviews (Coenye and Nelis 2010, Malone, et al. 2017).

Nanoscale cavitation nucleating agents such as nanodroplets and polymeric nanocups (Kwan, et al. 2015) could be interesting for sonobactericide as they could penetrate the biofilm, and help nucleate cavitation throughout the biofilm. In particular, the process of droplet vaporization may exert mechanical forces on the biofilm in addition to antibiotic activity (Guo, et al. 2017). Nanodroplets can nucleate sustained cavitation in closed fluid spaces (Chen, et al. 2013). Polymeric nanocups nucleate inertial cavitation activity with thresholds inversely proportional to size. For example, nanocups with mean size of 180 nm and 600 nm have been reported to nucleate inertial cavitation at peak rarefactional pressures of 3 MPa and 0.5 MPa, respectively (Kwan, et al. 2015). These agents have not yet been investigated for treating biofilms. Despite the potential advantages offered by nanodroplets and nanocups, these agents are not yet clinically approved, or readily available. Therefore, sonobactericide using these agents may not be clinically feasible in the near future.

Recalcitrant biofilms may be treated with shock waves (Gnanadhas, et al. 2015, Qi, et al. 2016) or histotripsy (Xu, et al. 2012, Bigelow, et al. 2017). Jetting from shock waves has been used in the clinic to destroy kidney and gallstones with lithotripsy (Vakil and Everbach 1993). Highly focused image-guided ultrasound beams can help concentrate acoustic energy at the biofilm site, while avoiding collateral damage. Histotripsy can be combined with a cavitation nucleation agent, such as phase-shift nanodroplets (Vlaisavljevich, et al. 2013) and echogenic liposomes (Bader, et al. 2016b) to lower the acoustic pressure thresholds for ablation, which could potentially improve the safety profile of treatment. Another potential application to treat biofilm infections harnessing sound is an ultrasonically activated stream. Birkin et al. (2015) demonstrated that by applying low-amplitude ultrasound (135 kHz, 120–250 kPa) through a liquid stream directed at a surface, endogenous cavitation nuclei can be activated at the solid/liquid interface enough to disrupt biofilm.

Combining ultrasound, cavitation nuclei and antibiotic therapy with matrix-degrading enzymes implicated in biofilm dispersal such as glycosidases, proteases, and deoxyribonucleases (Kaplan 2010, Zhu, et al. 2013, Li, et al. 2015) is a promising strategy for treating biofilms. Our group has recently reported the use of rt-PA, a clinically approved fibrinolytic agent, along with Definity® microbubbles, an antibiotic, and 120 kHz intermittent ultrasound for sonobactericide in an *in vitro* flow model (Lattwein, et al. 2018). This strategy could be promising for treating biofilms that have fibrin as a primary structural component. The microstreaming produced by cavitation nuclei (Kooiman, et al. 2014) can help remove biofilm degradation products and enhance the delivery of drugs, similar to sonothrombolysis studies (Bader, et al. 2016a). Although the feasibility of biofilm

dispersal has been demonstrated in previous studies (Kaplan 2010), more work needs to be done to elucidate the efficacy of combination therapy with matrix-degrading enzymes, ultrasound, and microbubbles. Future research could also include the interference of quorum sensing, which is bacterial communication that regulates several virulence pathways through signaling molecules and increases with cell density (Whiteley, et al. 2017). Because of the high potential of this envision approach, many compounds are under development that could be combined with sonobactericide to enhance efficacy (Fleitas Martínez, et al. 2019). In addition, it is unknown if sonobactericide has an effect on quorum sensing without these agents.

Safety and efficacy of sonobactericide are paramount. Accurate characterization of the acoustic fields (ter Haar, et al. 2011) and parameters used, standardization of protocols for the assessment of treatment efficacy, and development of *in vitro* and preclinical models that mimic the *in vivo* milieu will help accelerate the transition of sonobactericide to the clinic. In addition, enabling image guidance methods, such as active (Miller, et al. 2016) or passive cavitation imaging (Haworth, et al. 2017) and real-time feedback (Sun, et al. 2017) may help monitor treatment progress, standardize the acoustic dose, and aid in improving the safety and efficacy of *in situ* destruction of biofilms.

ACKNOWLEDGEMENTS

Financial support from the Erasmus MC Foundation (fellowship to KK) and the U.S. National Institutes of Health, National Institute of Neurological Disorders and Stroke grant R01 NS047603 (PI: CKH) is gratefully acknowledged.

REFERENCES

Agarwal A, Jern Ng W, Liu Y. Removal of biofilms by intermittent low-intensity ultrasonication triggered bursting of microbubbles. Biofouling 2014;30:359–65. [PubMed: 24571133]

Algburi A, Comito N, Kashtanov D, Dicks LMT, Chikindas ML. Control of biofilm formation: antibiotics and beyond. Appl Environ Microbiol 2017;83.

Alzaraa A, Gravante G, Chung WY, Al-Leswas D, Morgan B, Dennison A, Lloyd D. Contrast-enhanced ultrasound in the preoperative, intraoperative and postoperative assessment of liver lesions. Hepatol Res 2013;43:809–19. [PubMed: 23745715]

Anastasiadis P, Mojica KD, Allen JS, Matter ML. Detection and quantification of bacterial biofilms combining high-frequency acoustic microscopy and targeted lipid microparticles. J Nanobiotechnol 2014;12:24.

Apfel RE. Sonic effervescence: a tutorial on acoustic cavitation. J Acoust Soc Am 1997;101:1227–37.

Archer NK, Mazaitis MJ, Costerton JW, Leid JG, Powers ME, Shirtliff ME. Staphylococcus aureus biofilms: properties, regulation, and roles in human disease. Virulence 2011;2:445–59. [PubMed: 21921685]

Argenziano M, Banche G, Luganini A, Finesso N, Allizond V, Gulino GR, Khadjavi A, Spagnolo R, Tullio V, Giribaldi G, Guiot C, Cuffini AM, Prato M, Cavalli R. Vancomycin-loaded nanobubbles: A new platform for controlled antibiotic delivery against methicillin-resistant Staphylococcus aureus infections. Int J Pharm 2017;523:176–88. [PubMed: 28330735]

Azuma T, Kawabata K-i, Umemura S-i, Ogihara M, Kubota J, Sasaki A, Furuhata H. Bubble generation by standing wave in water surrounded by cranium with transcranial Ultrasonic Beam. Japn J Appl Phys 2005;44:4625–30.

Baddour LM, Wilson WR, Bayer AS, Fowler VG Jr., Tleyjeh IM, Rybak MJ, Barsic B, Lockhart PB, Gewitz MH, Levison ME, Bolger AF, Steckelberg JM, Baltimore RS, Fink AM, O'Gara P, Taubert KA, American Heart Association Committee on Rheumatic Fever E, Kawasaki Disease of

the Council on Cardiovascular Disease in the Young CoCCCoCS, Anesthesia, Stroke C. Infective endocarditis in adults: diagnosis, antimicrobial therapy, and management of complications: a scientific statement for Healthcare professionals from the American Heart Association. Circulation 2015;132:1435–86. [PubMed: 26373316]

Bader KB, Bouchoux G, Holland CK. Sonothrombolysis. Adv Exp Med Biol 2016a;880:339–62. [PubMed: 26486347]

Bader KB, Gruber MJ, Holland CK. Shaken and stirred: mechanisms of ultrasound-enhanced thrombolysis. Ultrasound Med Biol 2015;41:187–96. [PubMed: 25438846]

Bader KB, Haworth KJ, Shekhar H, Maxwell AD, Peng T, McPherson DD, Holland CK. Efficacy of histotripsy combined with rt-PA in vitro. Phys Med Biol 2016b;61:5253–74. [PubMed: 27353199]

Bader KB, Holland CK. Gauging the likelihood of stable cavitation from ultrasound contrast agents. Phys Med Biol 2013;58:127–44. [PubMed: 23221109]

Bæk KT, Frees D, Renzoni A, Barras C, Rodriguez N, Manzano C, Kelley WL. Genetic variation in the Staphylococcus aureus 8325 strain lineage revealed by whole-genome sequencing. PloS One 2013;8:e77122. [PubMed: 24098817]

Bigelow TA, Thomas CL, Wu H, Itani KMF. Histotripsy treatment of S. aureus biofilms on surgical mesh samples under varying pulse durations. IEEE Trans Ultrason Ferroelectr Freq Control 2017;64:1420–28. [PubMed: 28650808]

Birkin PR, Offin DG, Vian CJB, Howlin RP, Dawson JI, Secker TJ, Hervé RC, Stoodley P, Oreffo ROC, Keevil CW, Leighton TG. Cold water cleaning of brain proteins, biofilm and bone – harnessing an ultrasonically activated stream. Phys Chem Chem Phys 2015;17:20574–79. [PubMed: 26200694]

Bjarnsholt T, Alhede M, Alhede M, Eickhardt-Sørensen SR, Moser C, Kühl M, Jensen PØ, Høiby N. The in vivo biofilm. Trends Microbiol 2013;21:466–74. [PubMed: 23827084]

Black JJ, Yu FT, Schnatz RG, Chen X, Villanueva FS, Pacella JJ. Effect of thrombus composition and viscosity on sonoreperfusion efficacy in a model of micro-vascular obstruction. Ultrasound Med Biol 2016;42:2220–31. [PubMed: 27207018]

Brady RA, Mocca CP, Plaut RD, Takeda K, Burns DL. Comparison of the immune response during acute and chronic Staphylococcus aureus infection. PloS One 2018;13:e0195342–e42. [PubMed: 29596507]

Bröker BM, Holtfreter S, Bekeredjian-Ding I. Immune control of Staphylococcus aureus – regulation and counter-regulation of the adaptive immune response. Int J Med Microbiol 2014;304:204–14. [PubMed: 24462009]

Cai Y, Wang J, Liu X, Wang R, Xia L. A review of the combination therapy of low frequency ultrasound with antibiotics. BioMed Res Int 2017;2017:14.

Carli AV, Ross FP, Bhimani SJ, Nodzo SR, Bostrom MP. Developing a clinically representative model of periprosthetic joint infection. J Bone Joint Surg Am 2016;98:1666–76. [PubMed: 27707853]

Carmen JC, Nelson JL, Beckstead BL, Runyan CM, Robison RA, Schaalje GB, Pitt WG. Ultrasonic-enhanced gentamicin transport through colony biofilms of Pseudomonas aeruginosa and Escherichia coli. J Infect Chemother 2004;10:193–99. [PubMed: 15365858]

Carugo D, Owen J, Crake C, Lee JY, Stride E. Biologically and acoustically compatible chamber for studying ultrasound-mediated delivery of therapeutic compounds. Ultrasound Med Biol 2015;41:1927–37. [PubMed: 25922133]

Cavalieri F, Ashokkumar M, Grieser F, Caruso F. Ultrasonic synthesis of stable, functional lysozyme microbubbles. Langmuir 2008;24:10078–83. [PubMed: 18710266]

Cavalieri F, Micheli L, Kaliappan S, Teo BM, Zhou M, Palleschi G, Ashokkumar M. Antimicrobial and biosensing ultrasound-responsive lysozyme-shelled microbubbles. ACS Appl Mater Interfaces 2013;5:464–71. [PubMed: 23265433]

Cavalieri F, Zhou M, Tortora M, Lucilla B, Ashokkumar M. Methods of preparation of multifunctional microbubbles and their in vitro / in vivo assessment of stability, functional and structural properties. Curr Pharm Des 2012;18:2135–51. [PubMed: 22352769]

Chen CC, Sheeran PS, Wu S-Y, Olumolade OO, Dayton PA, Konofagou EE. Targeted drug delivery with focused ultrasound-induced blood-brain barrier opening using acoustically-activated nanodroplets. J Controlled Release 2013;172:795–804.

Chen H, Brayman AA, Evan AP, Matula TJ. Preliminary observations on the spatial correlation between short-burst microbubble oscillations and vascular bioeffects. Ultrasound Med Biol 2012;38:2151–62. [PubMed: 23069136]

Chen H, Kreider W, Brayman AA, Bailey MR, Matula TJ. Blood vessel deformations on microsecond time scales by ultrasonic cavitation. Phys Rev Lett 2011;106:034301. [PubMed: 21405276]

Chen WS, Matula TJ, Brayman AA, Crum LA. A comparison of the fragmentation thresholds and inertial cavitation doses of different ultrasound contrast agents. J Acoust Soc Am 2003;113:643–51. [PubMed: 12558300]

Chetty K, Stride E, Sennoga CA, Hajnal JV, Eckersley RJ. High-speed optical observations and simulation results of SonoVue microbubbles at low-pressure insonation. IEEE Trans Ultrason Ferroelectr Freq Control 2008;55:1333–42. [PubMed: 18599421]

Chomas JE, Dayton P, Allen J, Morgan K, Ferrara KW. Mechanisms of contrast agent destruction. IEEE Trans Ultrason Ferroelectr Freq Control 2001;48:232–48. [PubMed: 11367791]

Christiansen C, Kryvi H, Sontum PC, Skotland T. Physical and biochemical characterization of Albunex, a new ultrasound contrast agent consisting of air-filled albumin microspheres suspended in a solution of human albumin. Biotechnol Appl Biochem 1994;19:307–20. [PubMed: 8031506]

Chua SL, Liu Y, Yam JKH, Chen Y, Vejborg RM, Tan BGC, Kjelleberg S, Tolker-Nielsen T, Givskov M, Yang L. Dispersed cells represent a distinct stage in the transition from bacterial biofilm to planktonic lifestyles. Nat Commun 2014;5:4462. [PubMed: 25042103]

Coakley WT, Bardsley DW, Grundy MA, Zamani F, Clarke DJ. Cell manipulation in ultrasonic standing wave Ffelds. J Chem Technol Biotechnol 1989;44:43–62.

Coenye T, Nelis HJ. In vitro and in vivo model systems to study microbial biofilm formation. J Microbiol Methods 2010;83:89–105. [PubMed: 20816706]

Collis J, Manasseh R, Liovic P, Tho P, Ooi A, Petkovic-Duran K, Zhu Y. Cavitation microstreaming and stress fields created by microbubbles. Ultrasonics 2010;50:273–79. [PubMed: 19896683]

Conner-Kerr T, Alston G, Stovall A, Vernon T, Winter D, Meixner J, Grant K, Kute T. The effects of low-frequency ultrasound (35 kHz) on methicillin-resistant Staphylococcus aureus (MRSA) in vitro. Ostomy Wound Manag 2010;56:32–43.

Connolly KL, Roberts AL, Holder RC, Reid SD. Dispersal of group A streptococcal biofilms by the cysteine protease SpeB leads to increased disease severity in a murine model. PloS One 2011;6:e18984. [PubMed: 21547075]

Costerton JW, Stewart PS, Greenberg EP. Bacterial biofilms: a common cause of persistent infections. Science 1999;284:1318–22. [PubMed: 10334980]

Crosby HA, Kwiecinski J, Horswill AR. Staphylococcus aureus aggregation and coagulation mechanisms, and their function in host-pathogen interactions. Adv Appl Microbiol 2016;96:1–41. [PubMed: 27565579]

Dalecki D Mechanical bioeffects of ultrasound. Annu Rev Biomed Eng 2004;6:229–48. [PubMed: 15255769]

Deffieux T, Konofagou EE. Numerical study of a simple transcranial focused ultrasound system applied to blood-brain barrier opening. IEEE Trans Ultrason Ferroelectr Freq Control 2010;57:2637–53. [PubMed: 21156360]

DEFINITY®. US Food and Drug Administration 2011.

Delcaru C, Alexandru I, Podgoreanu P, Grosu M, Stavropoulos E, Chifiriuc CM, Lazar V. Microbial biofilms in urinary tract infections and prostatitis: etiology, pathogenicity, and combating strategies. Pathogens 2016;5.

Dhople V, Krukemeyer A, Ramamoorthy A. The human beta-defensin-3, an antibacterial peptide with multiple biological functions. Biochim Biophys Acta 2006;1758:1499–512. [PubMed: 16978580]

Dong Y, Chen S, Wang Z, Peng N, Yu J. Synergy of ultrasound microbubbles and vancomycin against Staphylococcus epidermidis biofilm. J Antimicrob Chemother 2013;68:816–26. [PubMed: 23248238]

Dong Y, Li J, Li P, Yu J. Ultrasound microbubbles enhance the activity of vancomycin against Staphylococcus epidermidis biofilms in vivo. J Ultrasound Med 2018;37:1379–87. [PubMed: 29159979]

Dong Y, Xu Y, Li P, Wang C, Cao Y, Yu J. Antibiofilm effect of ultrasound combined with microbubbles against Staphylococcus epidermidis biofilm. Int J Med Microbiol 2017;307:321–28. [PubMed: 28610835]

Elder SA. Cavitation Microstreaming. Journal Acoust Soc Am 1959;31:54–64.

Erriu M, Blus C, Szmukler-Moncler S, Buogo S, Levi R, Barbato G, Madonnaripa D, Denotti G, Piras V, Orru G. Microbial biofilm modulation by ultrasound: current concepts and controversies. Ultrason Sonochem 2014;21:15–22. [PubMed: 23751458]

Escoffre JM, Piron J, Novell A, Bouakaz A. Doxorubicin delivery into tumor cells with ultrasound and microbubbles. Mol Pharmaceutics 2011;8:799–806.

Estrela C, Estrela CR, Barbin EL, Spano JC, Marchesan MA, Pecora JD. Mechanism of action of sodium hypochlorite. Braz Dent J 2002;13:113–7. [PubMed: 12238801]

Faez T, Goertz D, De Jong N. Characterization of Definity ultrasound contrast agent at frequency range of 5–15 MHz. Ultrasound Med Biol 2011;37:338–42. [PubMed: 21257093]

Feinstein SB. New developments in ultrasonic contrast techniques: Transpulmonary passage of contrast agent and diagnostic implications. Echocardiography 1989;6:27–33.

Fleitas Martínez O, Rigueiras PO, Pires ÁdS, Porto WF, Silva ON, de la Fuente-Nunez C, Franco OL. Interference with quorum-sensing signal biosynthesis as a promising therapeutic strategy against multidrug-resistant pathogens. Front Cell Infect Microbiol 2019;8.

Forsberg F, Wu Y, Makin IR, Wang W, Wheatley MA. Quantitative acoustic characterization of a new surfactant-based ultrasound contrast agent. Ultrasound Med Biol 1997;23:1201–8. [PubMed: 9372569]

Fu Y-Y, Zhang L, Yang Y, Liu C-W, He Y-N, Li P, Yu X. Synergistic antibacterial effect of ultrasound microbubbles combined with chitosan-modified polymyxin B-loaded liposomes on biofilm-producing Acinetobacter baumannii. Int J Nanomed 2019;14:1805–15.

Fux CA, Stoodley P, Hall-Stoodley L, Costerton JW. Bacterial biofilms: a diagnostic and therapeutic challenge. Expert Rev Anti-infect Ther 2003;1:667–83. [PubMed: 15482163]

Gajdács M The concept of an ideal antibiotic: implications for drug design. Molecules 2019;24:892.

Gilboa-Garber N, Sudakevitz D. The hemagglutinating activities of Pseudomonas aeruginosa lectins PA-IL and PA-IIL exhibit opposite temperature profiles due to different receptor types. FEMS Immunol Med Microbiol 1999;25:365–69. [PubMed: 10497867]

Gnanadhas DP, Elango M, Janardhanraj S, Srinandan CS, Datey A, Strugnell RA, Gopalan J, Chakravortty D. Successful treatment of biofilm infections using shock waves combined with antibiotic therapy. Sci Rep 2015;5:17440–40. [PubMed: 26658706]

Goh BHT, Conneely M, Kneuper H, Palmer T, Klaseboer E, Khoo BC, Campbell P. High-speed imaging of ultrasound-mediated bacterial biofilm disruption. In: Lacković I, Vasic D (eds) 6th European Conference of the International Federation for Medical and Biological Enginnering proceedings. Springer Cham 2015;45:533–36.

Goldberg BB, Liu JB, Forsberg F. Ultrasound contrast agents: a review. Ultrasound Med Biol 1994;20:319–33. [PubMed: 8085289]

Gorce JM, Arditi M, Schneider M. Influence of bubble size distribution on the echogenicity of ultrasound contrast agents: a study of SonoVue. Invest Radiol 2000;35:661–71. [PubMed: 11110302]

Grant SS, Hung DT. Persistent bacterial infections, antibiotic tolerance, and the oxidative stress response. Virulence 2013;4:273–83. [PubMed: 23563389]

Guidi F, Vos HJ, Mori R, Jong ND, Tortoli P. Microbubble characterization through acoustically induced deflation. IEEE Trans Ultrason Ferroelectr Freq Control 2010;57:193–202. [PubMed: 20040446]

Guo H, Wang ZM, Du QY, Li P, Wang ZG, Wang AM. Stimulated phase-shift acoustic nanodroplets enhance vancomycin efficacy against methicillin-resistant Staphylococcus aureus biofilms. Int J Nanomed 2017;12:4679–90.

Habib G, Lancellotti P, Antunes MJ, Bongiorni MG, Casalta J-P, Del Zotti F, Dulgheru R, El Khoury G, Erba PA, Iung B, Miro JM, Mulder BJ, Plonska-Gosciniak E, Price S, Roos-Hesselink J, Snygg-Martin U, Thuny F, Tornos Mas P, Vilacosta I, Zamorano JL, Group ESD. 2015 ESC guidelines for the management of infective endocarditis: the task force for the management of

infective endocarditis of the European Society of Cardiology. Eur Heart J 2015;36:3075–128. [PubMed: 26320109]

Hajdu S, Holinka J, Reichmann S, Hirschl AM, Graninger W, Presterl E. Increased temperature enhances the antimicrobial effects of daptomycin, vancomycin, tigecycline, fosfomycin, and cefamandole on staphylococcal biofilms. Antimicrob Agents Chemother 2010;54:4078–84. [PubMed: 20679509]

Halford A, Ohl CD, Azarpazhooh A, Basrani B, Friedman S, Kishen A. Synergistic effect of microbubble emulsion and sonic or ultrasonic agitation on endodontic biofilm in vitro. J Endod 2012;38:1530–4. [PubMed: 23063230]

Han YW, Ikegami A, Chung P, Zhang L, Deng CX. Sonoporation is an efficient tool for intracellular fluorescent dextran delivery and one-step double-crossover mutant construction in Fusobacterium nucleatum. Appl Environ Microbiol 2007;73:3677–83. [PubMed: 17449701]

Han YW, Ikegami A, Rajanna C, Kawsar HI, Zhou Y, Li M, Sojar HT, Genco RJ, Kuramitsu HK, Deng CX. Identification and characterization of a novel adhesin unique to oral fusobacteria. J Bacteriol 2005;187:5330–40. [PubMed: 16030227]

Haworth KJ, Bader KB, Rich KT, Holland CK, Mast TD. Quantitative frequency-domain passive cavitation imaging. IEEE Trans Ultrason Ferroelectr Freq Control 2017;64:177–91. [PubMed: 27992331]

He N, Hu J, Liu H, Zhu T, Huang B, Wang X, Wu Y, Wang W, Qu D. Enhancement of vancomycin activity against biofilms by using ultrasound-targeted microbubble destruction. Antimicrob Agents Chemother 2011;55:5331–7. [PubMed: 21844319]

Helfield BL, Goertz DE. Nonlinear resonance behavior and linear shell estimates for Definity and MicroMarker assessed with acoustic microbubble spectroscopy. J Acoust Soc Am 2013;133:1158–68. [PubMed: 23363132]

Hensel K, Mienkina MP, Schmitz G. Analysis of ultrasound fields in cell culture wells for in vitro ultrasound therapy experiments. Ultrasound Med Biol 2011;37:2105–15. [PubMed: 22107908]

Hettiarachchi K, Talu E, Longo ML, Dayton PA, Lee AP. On-chip generation of microbubbles as a practical technology for manufacturing contrast agents for ultrasonic imaging. Lab Chip 2007;7:463–8. [PubMed: 17389962]

Holland CK, Apfel RE. An improved theory for the prediction of microcavitation thresholds. IEEE Trans Ultrason Ferroelectr Freq Control 1989;36:204–8. [PubMed: 18284969]

Horsley H, Owen J, Browning R, Carugo D, Malone-Lee J, Stride E, Rohn JL. Ultrasound-activated microbubbles as a novel intracellular drug delivery system for urinary tract infection. J Control Release 2019;301:166–75. [PubMed: 30904501]

Hu F, Zhu D, Wang F, Wang M. Current status and trends of antibacterial resistance in China. Clin Infect Dis 2018;67:S128–S34. [PubMed: 30423045]

Hu J, Zhang N Jr., Li L, Zhang N Sr., Ma Y, Zhao C, Wu Q, Li Y, He N, Wang X. The synergistic bactericidal effect of vancomycin on UTMD treated biofilm involves damage to bacterial cells and enhancement of metabolic activities. Sci Rep 2018;8:192. [PubMed: 29317687]

Huber TM, Beaver NM, Helps JR. Elimination of standing wave effects in ultrasound radiation force excitation in air using random carrier frequency packets. J Acoust Soc Am 2011;130:1838–43. [PubMed: 21973337]

Ikeda-Dantsuji Y, Feril LB Jr., Tachibana K, Ogawa K, Endo H, Harada Y, Suzuki R, Maruyama K. Synergistic effect of ultrasound and antibiotics against Chlamydia trachomatis-infected human epithelial cells in vitro. Ultrason Sonochem 2011;18:425–30. [PubMed: 20728399]

Jahan K, Balzer S, Mosto P. Toxicity of nonionic surfactants. Wit Trans Ecol Envir 2008;110:281-+.

Juffermans LJ, Dijkmans PA, Musters RJ, Visser CA, Kamp O. Transient permeabilization of cell membranes by ultrasound-exposed microbubbles is related to formation of hydrogen peroxide. Am J Physiol Heart Circ Physiol 2006;291:H1595–601. [PubMed: 16632548]

Kaplan JB. Biofilm dispersal: mechanisms, clinical implications, and potential therapeutic uses. J Dent Res 2010;89:205–18. [PubMed: 20139339]

Kim J, Lindsey BD, Chang W-Y, Dai X, Stavas JM, Dayton PA, Jiang X. Intravascular forward-looking ultrasound transducers for microbubble-mediated sonothrombolysis. Sci Rep 2017;7:3454. [PubMed: 28615645]

Kinsler LE, Frey AR, Coppens AB, Sanders JV. Fundamentals of Acoustics. New York: Wiley, 2000.

Kleven RT, Karani KB, Salido NG, Shekhar H, Haworth KJ, Mast TD, Tadessel DG, Holland CK. The effect of 220 kHz insonation scheme on rt-PA thrombolytic efficacy in vitro. Phys Med Biol 2019;64:165015. [PubMed: 31189149]

Koley D, Bard AJ. Triton X-100 concentration effects on membrane permeability of a single HeLa cell by scanning electrochemical microscopy (SECM). Proc Natl Acad Sci USA 2010;107:16783–7. [PubMed: 20837548]

Koo H, Allan RN, Howlin RP, Stoodley P, Hall-Stoodley L. Targeting microbial biofilms: current and prospective therapeutic strategies. Nat Rev Microbiol 2017;15:740–55. [PubMed: 28944770]

Kooiman K, Vos HJ, Versluis M, de Jong N. Acoustic behavior of microbubbles and implications for drug delivery. Adv Drug Deliv Rev 2014;72:28–48. [PubMed: 24667643]

Kripfgans OD, Fowlkes JB, Miller DL, Eldevik OP, Carson PL. Acoustic droplet vaporization for therapeutic and diagnostic applications. Ultrasound Med Biol 2000;26:1177–89. [PubMed: 11053753]

Kwan JJ, Myers R, Coviello CM, Graham SM, Shah AR, Stride E, Carlisle RC, Coussios CC. Ultrasound-propelled nanocups for drug delivery. Small 2015;11:5305–14. [PubMed: 26296985]

Kysela DT, Randich AM, Caccamo PD, Brun YV. Diversity takes shape: understanding the mechanistic and adaptive basis of bacterial morphology. PloS Biol 2016;14:e1002565. [PubMed: 27695035]

Lanjouw E, Ouburg S, de Vries H, Stary A, Radcliffe K, Unemo M. 2015 European guideline on the management of Chlamydia trachomatis infections. Int J STD AIDS 2016;27:333–48. [PubMed: 26608577]

Lattwein KR, Shekhar H, van Wamel WJB, Gonzalez T, Herr AB, Holland CK, Kooiman K. An in vitro proof-of-principle study of sonobactericide. Sci Rep 2018;8:3411. [PubMed: 29467474]

Lebeaux D, Ghigo JM, Beloin C. Biofilm-related infections: bridging the gap between clinical management and fundamental aspects of recalcitrance toward antibiotics. Microbiol Mol Biol Rev 2014;78:510–43. [PubMed: 25184564]

Lee SW, Gu H, Kilberg JB, Ren D. Sensitizing bacterial cells to antibiotics by shape recovery triggered biofilm dispersion. Acta Biomaterialia 2018;81:93–102. [PubMed: 30267885]

Leighton TG. The Acoustic Bubble. London: Academic Press, 1994.

Lewis K Persister cells and the riddle of biofilm survival. Biochem (Mosc) 2005;70:267–74.

Lewis K Platforms for antibiotic discovery. Nat Rev Drug Discov 2013;12:371. [PubMed: 23629505]

Li S, Zhu C, Fang S, Zhang W, He N, Xu W, Kong R, Shang X. Ultrasound microbubbles enhance human beta-defensin 3 against biofilms. J Surg Res 2015;199:458–69. [PubMed: 26119274]

Liao AH, Hung CR, Lin CF, Lin YC, Chen HK. Treatment effects of lysozyme-shelled microbubbles and ultrasound in inflammatory skin disease. Sci Rep 2017;7:41325. [PubMed: 28117399]

Liao X, Li J, Suo Y, Chen S, Ye X, Liu D, Ding T. Multiple action sites of ultrasound on Escherichia coli and Staphylococcus aureus. Food Sci Hum Wellness 2018;7:102–09.

Lin CY, Pitt WG. Acoustic droplet vaporization in biology and medicine. Biomed Res Int 2013;2013:404361. [PubMed: 24350267]

Lin T, Cai XZ, Shi MM, Ying ZM, Hu B, Zhou CH, Wang W, Shi ZL, Yan SG. In vitro and in vivo evaluation of vancomycin-loaded PMMA cement in combination with ultrasound and microbubbles-mediated ultrasound. Biomed Res Int 2015;2015:309739. [PubMed: 25632389]

Liu P, Wang X, Zhou S, Hua X, Liu Z, Gao Y. Effects of a novel ultrasound contrast agent with long persistence on right ventricular pressure: comparison with SonoVue. Ultrasonics 2011;51:210–4. [PubMed: 20825961]

Lumason®. US Food and Drug Administration 2016.

Madsen HH, Rasmussen F. Contrast-enhanced ultrasound in oncology. Cancer Imaging 2011;11 Spec No A:S167–73.

Magana M, Sereti C, Ioannidis A, Mitchell CA, Ball AR, Magiorkinis E, Chatzipanagiotou S, Hamblin MR, Hadjifrangiskou M, Tegos GP. Options and limitations in clinical investigation of bacterial biofilms. Clin Microbiol Rev 2018;31:e00084–16.

Mahalingam S, Xu Z, Edirisinghe M. Antibacterial activity and biosensing of PVA-lysozyme microbubbles formed by pressurized gyration. Langmuir 2015;31:9771–80. [PubMed: 26307462]

Mai-Prochnow A, Clauson M, Hong J, Murphy AB. Gram positive and Gram negative bacteria differ in their sensitivity to cold plasma. Sci Rep 2016;6:38610. [PubMed: 27934958]

Malone M, Goeres DM, Gosbell I, Vickery K, Jensen S, Stoodley P. Approaches to biofilm-associated infections: the need for standardized and relevant biofilm methods for clinical applications. Expert Rev Anti-infect Ther 2017;15:147–56. [PubMed: 27858472]

Mandell LA, Marrie TJ, Grossman RF, Chow AW, Hyland RH, Group at CC-APW. Canadian guidelines for the initial management of community-acquired pneumonia: an evidence-based update by the Canadian Infectious Diseases Society and the Canadian Thoracic Society. Clin Infect Dis 2000;31:383–421. [PubMed: 10987698]

Mannaris C, Averkiou MA. Investigation of microbubble response to long pulses used in ultrasound-enhanced drug delivery. Ultrasound Med Biol 2012;38:681–91. [PubMed: 22341047]

Marks LR, Davidson BA, Knight PR, Hakansson AP. Interkingdom signaling induces Streptococcus pneumoniae biofilm dispersion and transition from asymptomatic colonization to disease. MBio 2013;4:e00438–13. [PubMed: 23882016]

Maurice NM, Bedi B, Sadikot RT. Pseudomonas aeruginosa biofilms: host response and clinical implications in lung infections. Am J Respir Cell Mol Biol 2018;58:428–39. [PubMed: 29372812]

Mayer S, Grayburn PA. Myocardial contrast agents: recent advances and future directions. Prog Cardiovasc Dis 2001;44:33–44. [PubMed: 11533925]

McConoughey SJ, Howlin R, Granger JF, Manring MM, Calhoun JH, Shirtliff M, Kathju S, Stoodley P. Biofilms in periprosthetic orthopedic infections. Future Microbiol 2014;9:987–1007. [PubMed: 25302955]

Menozzi G, Maccabruni V, Gabbi E. Left kidney infarction in a patient with native aortic valve infective endocarditis: diagnosis with contrast-enhanced ultrasound. J Ultrasound 2013a;16:145–6. [PubMed: 24432168]

Menozzi G, Maccabruni V, Gabbi E, Leone N, Calzolari M. Contrast-enhanced ultrasound evaluation of splenic embolization in patients with definite left-sided infective endocarditis. Ultrasound Med Biol 2013b;39:2205–10. [PubMed: 23969166]

Mermel LA, Allon M, Bouza E, Craven DE, Flynn P, O'Grady NP, Raad II, Rijnders BJA, Sherertz RJ, Warren DK. Clinical practice guidelines for the diagnosis and management of intravascular catheter-related infection: 2009 update by the Infectious Diseases Society of America. Clin Infect Dis 2009;49:1–45. [PubMed: 19489710]

Miller RM, Zhang X, Maxwell AD, Cain CA, Xu Z. Bubble-induced color doppler feedback for histotripsy tissue fractionation. IEEE Trans Ultrason Ferroelectr Freq Control 2016;63:408–19. [PubMed: 26863659]

Moran CM, Watson RJ, Fox KA, McDicken WN. In vitro acoustic characterisation of four intravenous ultrasonic contrast agents at 30 MHz. Ultrasound Med Biol 2002;28:785–91. [PubMed: 12113791]

Nishikawa T, Yoshida A, Khanal A, Habu M, Yoshioka I, Toyoshima K, Takehara T, Nishihara T, Tachibana K, Tominaga K. A study of the efficacy of ultrasonic waves in removing biofilms. Gerodontology 2010;27:199–206. [PubMed: 20491951]

Nolsoe CP, Lorentzen T. International guidelines for contrast-enhanced ultrasonography: ultrasound imaging in the new millennium. Ultrasonography 2016;35:89–103. [PubMed: 26867761]

Nyborg WL. Acoustic streaming due to attenuated plane waves. J Acoust Soc Am 1953;25:68–75.

O'Reilly MA, Huang Y, Hynynen K. The impact of standing wave effects on transcranial focused ultrasound disruption of the blood-brain barrier in a rat model. Phys Med Biol 2010;55:5251–67. [PubMed: 20720286]

Oberbach A, Schlichting N, Feder S, Lehmann S, Kullnick Y, Buschmann T, Blumert C, Horn F, Neuhaus J, Neujahr R, Bagaev E, Hagl C, Pichlmaier M, Rodloff AC, Graber S, Kirsch K, Sandri M, Kumbhari V, Behzadi A, Behzadi A, Correia JC, Mohr FW, Friedrich M. New insights into valve-related intramural and intracellular bacterial diversity in infective endocarditis. PloS One 2017;12:e0175569. [PubMed: 28410379]

Odekerken JCE, Logister DMW, Assabre L, Arts JJC, Walenkamp GHIM, Welting TJM. ELISA-based detection of gentamicin and vancomycin in protein-containing samples. SpringerPlus 2015;4:614. [PubMed: 26543749]

Ohl SW, Klaseboer E, Khoo BC. Bubbles with shock waves and ultrasound: a review. Interface Focus 2015;5:20150019. [PubMed: 26442143]

Okshevsky M, Meyer RL. Evaluation of fluorescent stains for visualizing extracellular DNA in biofilms. J Microbiol Methods 2014;105:102–4. [PubMed: 25017901]

Olson ME, Ceri H, Morck DW, Buret AG, Read RR. Biofilm bacteria: formation and comparative susceptibility to antibiotics. Can J Vet Res 2002;66:86–92. [PubMed: 11989739]

OPTISONTM. US Food and Drug Administration 2012.

Osmon DR, Berbari EF, Berendt AR, Lew D, Zimmerli W, Steckelberg JM, Rao N, Hanssen A, Wilson WR. Diagnosis and management of prosthetic joint infection: clinical practice guidelines by the infectious diseases society of America. Clin Infect Dis 2012;56:e1–e25. [PubMed: 23223583]

Otto M Staphylococcal biofilms. Curr Top Microbiol Immunol 2008;322:207–28. [PubMed: 18453278]

Overvelde M, Garbin V, Dollet B, de Jong N, Lohse D, Versluis M. Dynamics of coated microbubbles adherent to a wall. Ultrasound Med Biol 2011;37:1500–08. [PubMed: 21816289]

Owens CA. Ultrasound-enhanced thrombolysis: EKOS endowave infusion catheter system. Semin Intervent Radiol 2008;25:37–41. [PubMed: 21326491]

Parini MR, Pitt WG. Dynamic removal of oral biofilms by bubbles. Colloids Surf B Biointerfaces 2006;52:39–46. [PubMed: 16870403]

Pitt WG, McBride MO, Lunceford JK, Roper RJ, Sagers RD. Ultrasonic enhancement of antibiotic action on gram-negative bacteria. Antimicrob Agents Chemother 1994;38:2577–82. [PubMed: 7872751]

Postema M, Bouakaz A, Chien Ting C, Jong Nd. 2002 Optically observed microbubble coalescence and collapse. 2002 IEEE Ultrasonics Symposium, 2002. Proceedings, 1949–52 vol.2.

Qi X, Zhao Y, Zhang J, Han D, Chen C, Huang Y, Chen X, Zhang X, Wang T, Li X. Increased effects of extracorporeal shock waves combined with gentamicin against Staphylococcus aureus biofilms in vitro and in vivo. Ultrasound Med Biol 2016;42:2245–52. [PubMed: 27260244]

Roberts AEL, Kragh KN, Bjarnsholt T, Diggle SP. The limitations of in vitro experimentation in understanding biofilms and chronic infection. J Mol Biol 2015;427:3646–61. [PubMed: 26344834]

Ronan E, Edjiu N, Kroukamp O, Wolfaardt G, Karshafian R. USMB-induced synergistic enhancement of aminoglycoside antibiotics in biofilms. Ultrasonics 2016;69:182–90. [PubMed: 27111871]

Rosenthal I, Sostaric JZ, Riesz P. Sonodynamic therapy—a review of the synergistic effects of drugs and ultrasound. Ultrason Sonochem 2004;11:349–63. [PubMed: 15302020]

Schneider M, Anantharam B, Arditi M, Bokor D, Broillet A, Bussat P, Fouillet X, Frinking P, Tardy I, Terrettaz J, Senior R, Tranquart F. BR38, a new ultrasound blood pool agent. Invest Radiol 2011;46:486–94. [PubMed: 21487303]

Schneider M, Arditi M, Barrau MB, Brochot J, Broillet A, Ventrone R, Yan F. BR1: a new ultrasonographic contrast agent based on sulfur hexafluoride-filled microbubbles. Invest Radiol 1995;30:451–7. [PubMed: 8557510]

Sharma PK, Gibcus MJ, van der Mei HC, Busscher HJ. Influence of fluid shear and microbubbles on bacterial detachment from a surface. Appl Environ Microbiol 2005;71:3668–73. [PubMed: 16000775]

Shen Y, Stojicic S, Qian W, Olsen I, Haapasalo M. The synergistic antimicrobial effect by mechanical agitation and two chlorhexidine preparations on biofilm bacteria. J Endod 2010;36:100–04. [PubMed: 20003944]

Shi A, Min Y, Wan M. Flowing microbubble manipulation in blood vessel phantom using ultrasonic standing wave with stepwise frequency. Appl Phys Lett 2013;103:174105.

Shi WT, Forsberg F, Tornes A, Østensen J, Goldberg BB. Destruction of contrast microbubbles and the association with inertial cavitation. Ultrasound Med Biol 2000;26:1009–19. [PubMed: 10996701]

Short FL, Murdoch SL, Ryan RP. Polybacterial human disease: the ills of social networking. Trends Microbiol 2014;22:508–16. [PubMed: 24938173]

Silhavy TJ, Kahne D, Walker S. The bacterial cell envelope. Cold Spring Harb Perspect Biol 2010;2:a000414. [PubMed: 20452953]

Smeenge M, Tranquart F, Mannaerts CK, de Reijke TM, van de Vijver MJ, Laguna MP, Pochon S, de la Rosette JJMCH, Wijkstra H. First-in-human ultrasound molecular imaging with a VEGFR2-specific ultrasound molecular contrast agent (BR55) in prostate cancer: a safety and feasibility pilot study. Invest Radiol 2017;52:419–27. [PubMed: 28257340]

Song KH, Fan AC, Hinkle JJ, Newman J, Borden MA, Harvey BK. Microbubble gas volume: A unifying dose parameter in blood-brain barrier opening by focused ultrasound. Theranostics 2017;7:144–52. [PubMed: 28042323]

Sontum PC. Physicochemical characteristics of Sonazoid, a new contrast agent for ultrasound imaging. Ultrasound Med Biol 2008;34:824–33. [PubMed: 18255220]

Stewart PS, William Costerton J. Antibiotic resistance of bacteria in biofilms. The Lancet 2001;358:135–38.

Sugiyama MG, Mintsopoulos V, Raheel H, Goldenberg NM, Batt JE, Brochard L, Kuebler WM, Leong-Poi H, Karshafian R, Lee WL. Lung ultrasound and microbubbles enhance aminoglycoside efficacy and delivery to the lung in Escherichia coli–induced pneumonia and acute respiratory distress syndrome. Am J Respir Crit Care Med 2018;198:404–08. [PubMed: 29638143]

Sun T, Zhang Y, Power C, Alexander PM, Sutton JT, Aryal M, Vykhodtseva N, Miller EL, McDannold NJ. Closed-loop control of targeted ultrasound drug delivery across the blood-brain/tumor barriers in a rat glioma model. Proc Natl Acad Sci USA 2017;114:E10281–E90. [PubMed: 29133392]

Sutton JT, Haworth KJ, Pyne-Geithman G, Holland CK. Ultrasound-mediated drug delivery for cardiovascular disease. Expert Opin Drug Deliv 2013;10:573–92. [PubMed: 23448121]

Tandiono T, Ow DS, Driessen L, Chin CS, Klaseboer E, Choo AB, Ohl SW, Ohl CD. Sonolysis of Escherichia coli and Pichia pastoris in microfluidics. Lab Chip 2012;12:780–6. [PubMed: 22183135]

ter Haar G Safety and bio-effects of ultrasound contrast agents. Med Biol Eng Comput 2009;47:893–900. [PubMed: 19597745]

ter Haar G Ultrasound bioeffects and safety. Proc Inst Mech Eng H: J Eng Med 2010;224:363–73.

ter Haar G, Shaw A, Pye S, Ward B, Bottomley F, Nolan R, Coady A-M. Guidance on reporting ultrasound exposure conditions for bio-effects studies. Ultrasound Med Biol 2011;37:177–83. [PubMed: 21257086]

Thomen P, Robert J, Monmeyran A, Bitbol A-F, Douarche C, Henry N. Bacterial biofilm under flow: first a physical struggle to stay, then a matter of breathing. PloS One 2017;12:e0175197–e97. [PubMed: 28403171]

Vakil N, Everbach EC. Transient acoustic cavitation in gallstone fragmentation: A study of gallstones fragmented in vivo. Ultrasound Med Biol 1993;19:331–42. [PubMed: 8346607]

van Oosten M, Hahn M, Crane LMA, Pleijhuis RG, Francis KP, van Dijl JM, van Dam GM. Targeted imaging of bacterial infections: advances, hurdles and hopes. FEMS Microbiol Rev 2015;39:892–916. [PubMed: 26109599]

van Rooij T, Beekers I, Lattwein KR, van der Steen AFW, de Jong N, Kooiman K. Vibrational responses of bound and nonbound targeted lipid-coated single microbubbles. IEEE Trans Ultrason Ferroelectr Freq Control 2017;64:785–97. [PubMed: 28287967]

van Rooij T, Daeichin V, Skachkov I, de Jong N, Kooiman K. Targeted ultrasound contrast agents for ultrasound molecular imaging and therapy. Int Journal Hyperthermia 2015;31:90–106.

Vlaisavljevich E, Durmaz YY, Maxwell A, Elsayed M, Xu Z. Nanodroplet-mediated histotripsy for image-guided targeted ultrasound cell ablation. Theranostics 2013;3:851–64. [PubMed: 24312155]

Vollmer AC, Kwakye S, Halpern M, Everbach EC. Bacterial stress responses to 1-megahertz pulsed ultrasound in the presence of microbubbles. Appl Environ Microbiol 1998;64:3927–31. [PubMed: 9758821]

Vyas N, Manmi K, Wang Q, Jadhav AJ, Barigou M, Sammons RL, Kuehne SA, Walmsley AD. Which parameters affect biofilm removal with acoustic cavitation? A review. Ultrasound Med Biol 2019; 45:1044–55. [PubMed: 30792088]

Wang M, Zhang Y, Cai C, Tu J, Guo X, Zhang D. Sonoporation-induced cell membrane permeabilization and cytoskeleton disassembly at varied acoustic and microbubble-cell parameters. Sci Rep 2018;8:3885–85. [PubMed: 29497082]

Wang S, Hossack JA, Klibanov AL. Targeting of microbubbles: contrast agents for ultrasound molecular imaging. J Drug Target 2018;26:420–34. [PubMed: 29258335]

Ward M, Wu J, Chiu JF. Experimental study of the effects of Optison concentration on sonoporation in vitro. Ultrasound Med Biol 2000;26:1169–75. [PubMed: 11053752]

Wei K Contrast echocardiography: applications and limitations. Cardiol Rev 2012;20:25–32. [PubMed: 22143282]

Werdan K, Dietz S, Loffler B, Niemann S, Bushnaq H, Silber RE, Peters G, Muller-Werdan U. Mechanisms of infective endocarditis: pathogen-host interaction and risk states. Nat Rev Cardiol 2014;11:35–50. [PubMed: 24247105]

Whiteley M, Diggle SP, Greenberg EP. Progress in and promise of bacterial quorum sensing research. Nature 2017;551:313–20. [PubMed: 29144467]

Willmann JK, Bonomo L, Carla Testa A, Rinaldi P, Rindi G, Valluru KS, Petrone G, Martini M, Lutz AM, Gambhir SS. Ultrasound molecular imaging with BR55 in patients with breast and ovarian lesions: first-in-human results. J Clin Oncol 2017;35:2133–40. [PubMed: 28291391]

Xu J, Bigelow TA, Halverson LJ, Middendorf JM, Rusk B. Minimization of treatment time for in vitro 1.1 MHz destruction of Pseudomonas aeruginosa biofilms by high-intensity focused ultrasound. Ultrasonics 2012;52:668–75. [PubMed: 22341761]

Yi S, Han G, Shang Y, Liu C, Cui D, Yu S, Liao B, Ao X, Li G, Li L. Microbubble-mediated ultrasound promotes accumulation of bone marrow mesenchymal stem cell to the prostate for treating chronic bacterial prostatitis in rats. Sci Rep 2016;6:19745. [PubMed: 26797392]

Yu L, Zhong M, Wei Y. Direct fluorescence polarization assay for the detection of glycopeptide antibiotics. Anal Chem 2010;82:7044–48. [PubMed: 20704393]

Zapotoczna M, O'Neill E, O'Gara JP. Untangling the diverse and redundant mechanisms of Staphylococcus aureus biofilm formation. PLoS Pathog 2016;12:e1005671. [PubMed: 27442433]

Zhou H, Fang S, Kong R, Zhang W, Wu K, Xia R, Shang X, Zhu C. Effect of low frequency ultrasound plus fluorescent composite carrier in the diagnosis and treatment of methicillin-resistant staphylococcus aureus biofilm infection of bone joint implant. Int J Clin Exp Med 2018;11:799–805.

Zhou M, Cavalieri F, Ashokkumar M. Modification of the size distribution of lysozyme microbubbles using a post-sonication technique. Instrum Sci Technol 2012;40:51–60.

Zhu C, He N, Cheng T, Tan H, Guo Y, Chen D, Cheng M, Yang Z, Zhang X. Ultrasound-targeted microbubble destruction enhances human beta-defensin 3 activity against antibiotic-resistant Staphylococcus biofilms. Inflammation 2013;36:983–96. [PubMed: 23519963]

Zhu HX, Cai XZ, Shi ZL, Hu B, Yan SG. Microbubble-mediated ultrasound enhances the lethal effect of gentamicin on planktonic Escherichia coli. Biomed Res Int 2014;2014:142168. [PubMed: 24977141]

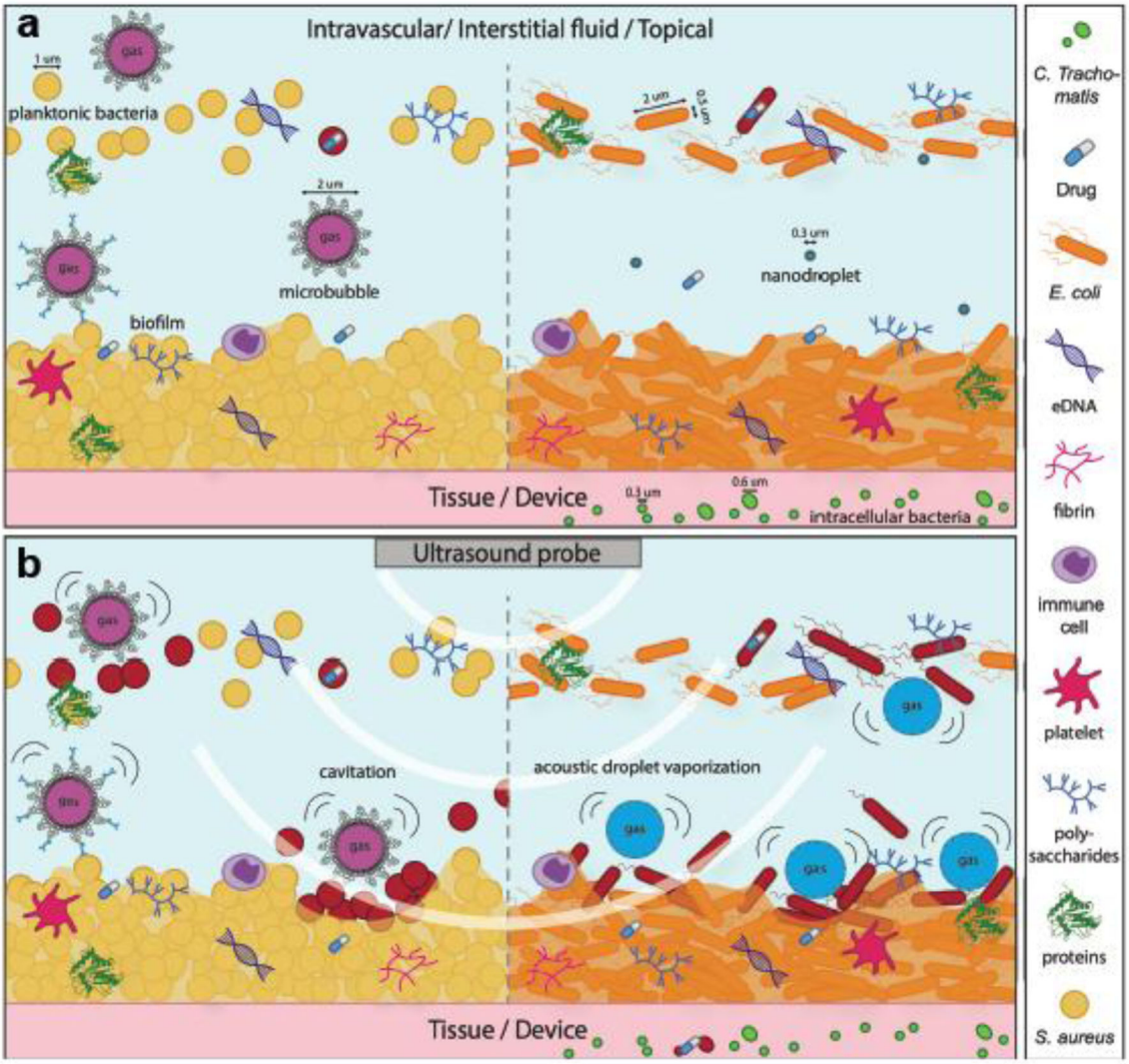

Figure 1.

Concept of sonobactericide (not drawn to scale). a) potential infection environments before ultrasound. Sizing of bacteria and cavitation nuclei are denoted with a line and an arrow on each end. b) ultrasound application where upon cavitating microbubbles and activated nanodroplets disrupt bacteria and biofilm composition. Bacteria that have become red in b) are considered dead or to have compromised membranes due to the effects from ultrasound and cavitating nuclei.

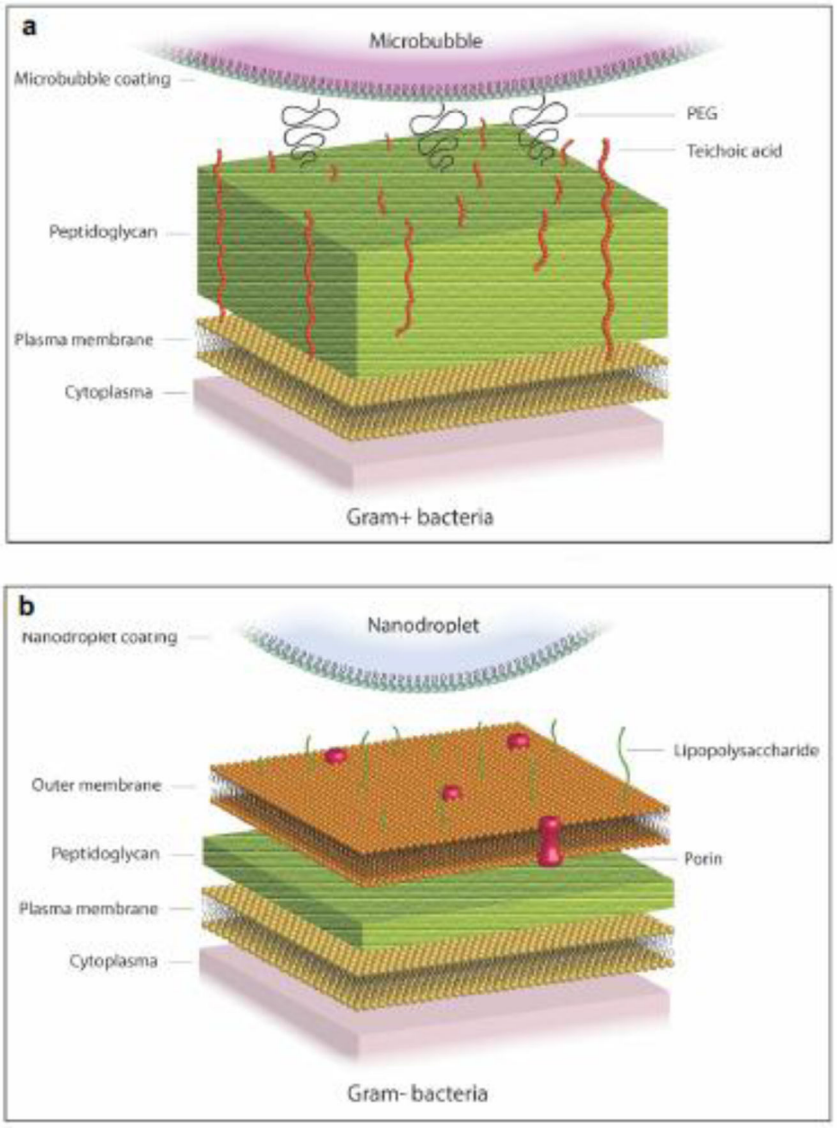

Figure 2.

Interaction of cavitation nuclei with bacteria: a) interaction between phospholipid-coated microbubble and Gram+ bacteria, b) interaction between phospholipid-coated nanodroplets and Gram− bacteria. PEG = polyethylene glycol.

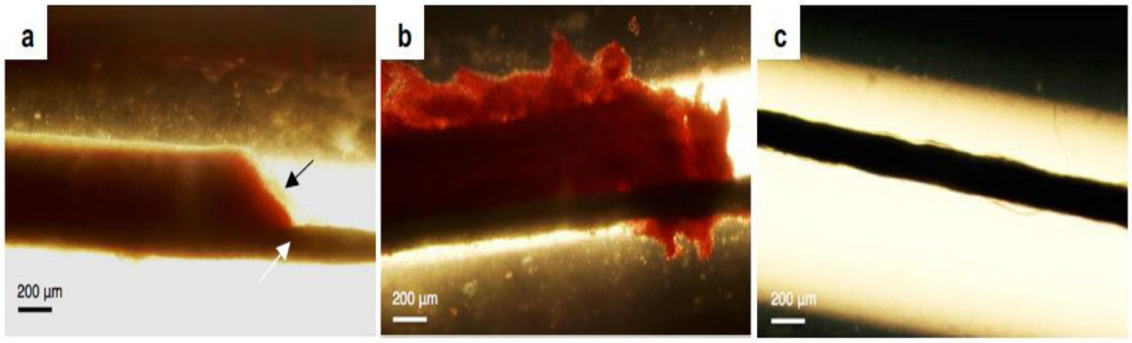

Figure 3.

Bright-field micrographs of *in vitro* produced *Staphylococcus aureus* infected clots following 30-min treatment with a) plasma alone, b) plasma, rt-PA (thrombolytic), and oxacillin (antibiotic), and c) plasma, rt-PA, oxacillin, ultrasound, and Definity® (microbubble). The black arrow in image a) indicates the biofilm (beige). The thick black line, seen in all images and denoted by a white arrow in image a), is the suture to which the respective infected clots were adhered. Ultrasound parameters were 0.12 MHz and 0.44 MPa peak-to-peak pressure, intermittent (50 seconds on, 30 seconds off) continuous wave for 30 minutes (reprinted (adapted) with permission from Lattwein et al. (2017)).

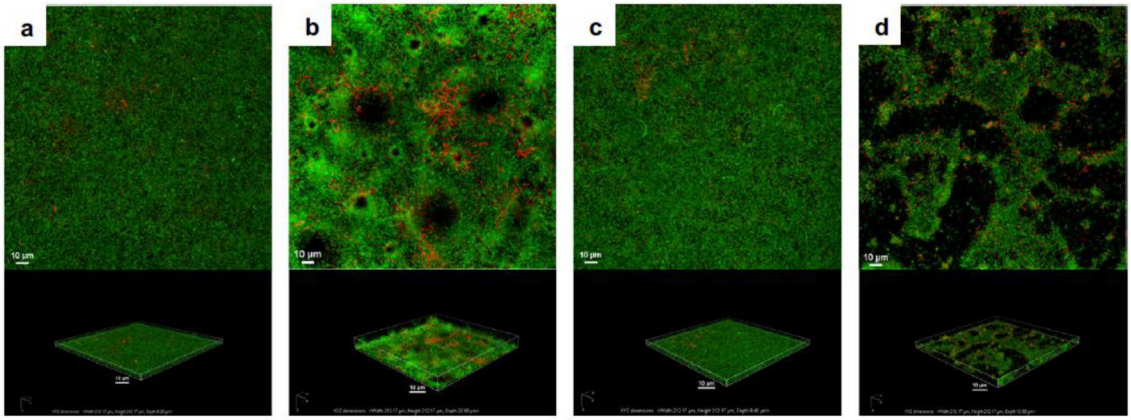

Figure 4.

Confocal laser scanning micrographs of *in vitro*, propidium iodide (red) stained, *Pseudomonas aeruginosa* PAO1:gfp-2 biofilms following treatment with a) nothing (control), b) ultrasound and Definity® (microbubble), c) gentamicin (antibiotic) alone, and d) gentamicin, ultrasound, and Definity®. The top panel is the top-down maximum intensity projection and the bottom panel is the corresponding three-dimensional volume rendering. Ultrasound parameters were 0.5 MHz at 1.1 MPa peak negative pressure with a 16-cycle tone burst and pulse repetition frequency of 1 kHz for 5 minutes (reprinted with permission from Ronan et al. (2016)).

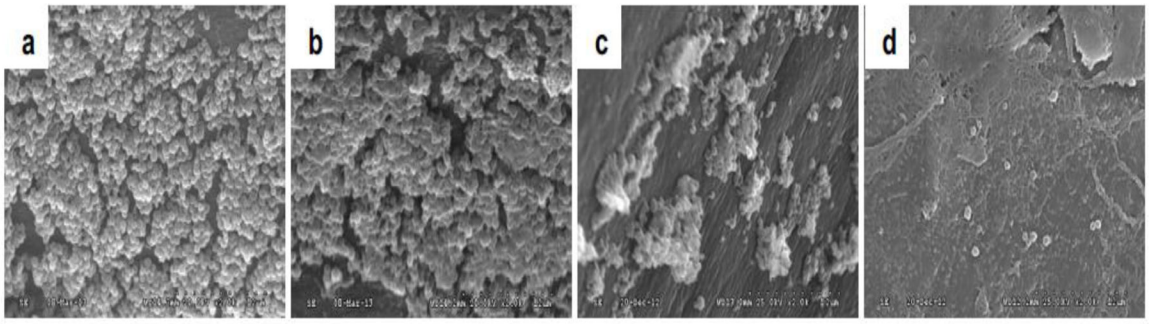

Figure 5.

Scanning electron micrographs of *Staphylococcus epidermidis* biofilms from subcutaneously implanted catheters in rabbits following treatment with a) nothing (control), b) ultrasound and a custom-made microbubble, c) vancomycin (antibiotic) alone, and d) vancomycin, ultrasound, and custom-made microbubble (original magnification × 2000). Ultrasound parameters were 0.3 MHz and 0.5 W/cm2 (or 0.12 MPa) with a 50% duty cycle for a total of 20 minutes (5 minutes twice a day) (reprinted (adapted) with permission from Dong et al. (2018)).

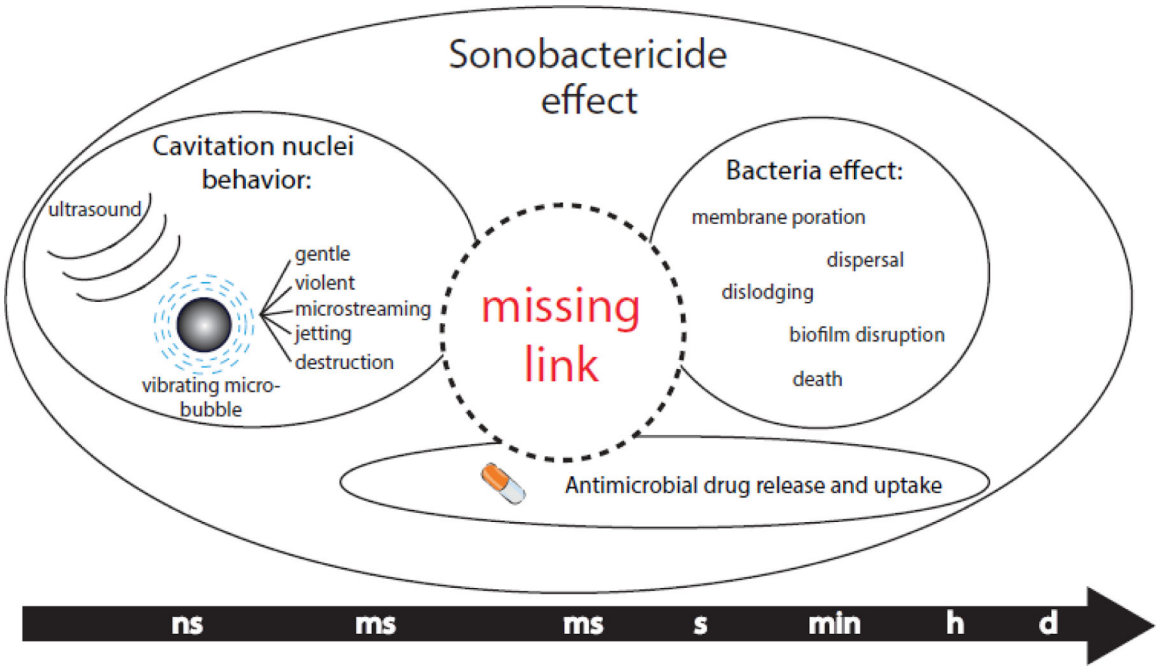

Figure 6.
Different time scales of the therapeutic effects of sonobactericide.

Table 1.

Overview of sonobactericide papers

Pathogen Type	Pathogen	Culture type	in vitro	In vivo	Model set-up	Antimicrobial	Cavitation nuclei	US frequency (MHz)	Pressure/ Intensity or calculated pressure	Cycles/PRF/ Treatment time	Ref
Gram+	*E. faecalis*	biofilm	x	-	root canals of single-rooted polymer and human teeth	5.25% NaOCl	custom-made	0.032 ± 0.004	N.D.	N.D., 1 min	(Halford, et al. 2012)
		intracellular	x	-	Infected human bladder cell organoid model	gentamicin	custom-made	1.1	2.5MPa	25% duty cycle, PRF 50 Hz, 20 s	(Horsley, et al. 2019)
	P. acnes	planktonic; *in vivo*: N.D.	x	x	eppendorf tube; intradermally into mouse ears	lysozyme	custom-made	1	*in vitro*: 1, 2, 3 W/cm^2 *in vivo*: 3 W/cm^2	50% duty cycle, *in vitro*: 1 min; *in vivo*: 1 min, q.d. for 13 d	(Liao, et al. 2017)
	S. aureus	planktonic	x	x	tissue culture plate; bone cement in rabbit tibiae	vancomycin	SonoVue	1	0.3 W/cm^2	30% duty cycle, 24 h	(Lin, et al. 2015)
		biofilm	x	-	tissue culture plate/coverslip	vancomycin	custom-made	1	0.3 W/cm^2	50% duty cycle, 5 min	(Guo, et al. 2017)
		biofilm	x	-	infected clot on a suture in glass capillaries	oxacillin	Definity	0.12	0.44 MPa (PTP)	continuous wave, 50 s on 30 s off, 30 min	(Lattwein, et al. 2018)
		biofilm	x	-	Subcutaneously implanted titanium plate in mice	human β-defensin 3	custom-made / SonoVue	0.08	0.2 W/cm^2	50% duty cycle, 20 min, t.i.d. for 7, 14, 28 d	(Zhou, et al. 2018)
	S. epidermidis	biofilm	x	x	tissue culture plate; subcutaneously implanted disk in rabbits	vancomycin	SonoVue	0.08	*in vitro*: 1 W/cm^2 *in vivo*: 0.5 W/cm^2	50% duty cycle, *in vitro*: 10 min; *in vivo*: 20 min, t.i.d. for 72 h	(He, et al. 2011)
		biofilm	x	-	OptiCell	vancomycin	custom-made	0.3	0.5 W/cm^2 or 0.12 MPa *	50% duty cycle, 5 min	(Dong, et al. 2013)
		biofilm	x	-	OptiCell	vancomycin	custom-made	1	0.5 W/cm^2 or 0.12 MPa *	50% duty cycle, 5 min	(Dong, et al. 2017)
		biofilm	-	x	Subcutaneously implanted catheter in rabbits	vancomycin	custom-made	0.3	0.5 W/cm^2 or 0.12 MPa *	50% duty cycle, 5 min, b.i.d. for 48 h	(Dong, et al. 2018)
		biofilm	x	-	tissue culture plate; glass FluoroDish	vancomycin	SonoVue	1	1 W/cm^2 or 0.24 MPa *	50% duty cycle, 10 min	(Hu, et al. 2018)

Pathogen Type	Pathogen	Culture type	in vitro	In vivo	Model set-up	Antimicrobial	Cavitation nuclei	US frequency (MHz)	Pressure/ Intensity or calculated pressure	Cycles/PRF/ Treatment time	Ref
Gram−	S. aureus & *S. epidermidis*	biofilm	x	-	tissue culture plate with titanium plate	human β-defensin 3	SonoVue	1	1 W/cm^2	50% duty cycle, 10 min	
		biofilm	-	x	subcutaneously implanted titanium plate in mice	human β-defensin 3	SonoVue	0.08	0.2 W/cm^2	50% duty cycle, 20 min, t.i.d. for 48 h	(Li, et al. 2015)
	S. mutans	biofilm	x	-	tissue culture plate with disk	none	Sonazoid	0.28	N.D.	0–90% duty cycle, 1 min	(Nishikawa, et al. 2010)
	A. *baumannii*	biofilm	x	-	tissue culture plate/coverslip	polymyxin B	custom-made	1	3 W/cm^2	continuous wave, 5 min	(Fu, et al. 2019)
	C. trachohmatis	intracellular	x	-	infected HeLa cells in tissue plate with gas permeable bottom	doxycycline; ceftizoxime	custom-made	1.011	0.15, 0.44 W/cm^2 or 0.13, 0.23 MPa$^{\#}$	25% duty cycle, 20 sec	(Ikeda-Dantsuji, et al. 2011)
	E. coli	planktonic	x	-	centrifuge tubes	none	Albunex; ST68 custom-made	1	500 W/cm2	1 ms pulse, PRF 20 Hz, 5 min	(Vollmer, et al. 1998)
		planktonic	x	-	tubes	gentamicin	SonoVue	0.0465	0.01 W/cm^2	33% duty cycle, 12 h	(Zhu, et al. 2014)
		N.D.	-	x	direct injection into rat prostates	none	custom-made	1	0.5 MPa/ 0.023 W/cm^2	1% duty cycle, 5 min	(Yi, et al. 2016)
		N.D.	-	x	Intratracheally infected mice	gentamicin	Definity	1.3	0.9 – 1.2 MPa (PNP)	pulse every 5 s, 5 min	(Sugiyama, et al. 2018)
	F. nucleatum	planktonic	x	-	tissue culture plate	none	Optison	0.96	0.5 MPa (PPP)	50% duty cycle, PRF 1 Hz, 90 s	(Han, et al. 2005)
		planktonic	x	-	tissue culture plate	none	Definity	1	0.25, 0.5, >0.9 MPa (PPP)	0 −50% duty cycle, PRF 1–100 Hz, 10, 90, 450 s	(Han, et al. 2005)
	P. aeruginosa	biofilm	x	-	glass coverslip in flow cell	gentamicin; streptomycin	Definity	0.5	1.1 MPa (PNP)	16 cycle tone burst, PRF 1 kHz, 5 min	(Ronan, et al. 2016)
	P. putida	biofilm	x	-	glass coverslip in acetate film chamber	none	SonoVue	0.25, 1	0.1, 0.5, 0.7 MPa (PNP)	50 μs pulse	(Goh, et al. 2015)
	E. coli & *P. pastoris* - (yeast)	planktonic	x	-	microfluidic system	none	custom-made	0.13	10 bar (~1 MPa)	500–50,000 cycles, ms – s, every 5 s	(Tandiono, et al. 2012)
Mixed	N.D.	biofilm	x	-	nylon membrane surface	none	custom-made	0.042	N.D.	2 sec pulse, every 2 min, 15 min	(Agarwal, et al. 2014)

US = ultrasound; PRF = pulse repetition frequency; N.D. = not defined; PTP = peak-to-peak pressure; PPP = peak positive pressure; PNP = peak negative pressure; q.d. = once a day; b.i.d. = twice a day; t.i.d. = thrice a day

* = calculated peak pressure from spatial pulse-average intensity (I_{SPTA}) values obtained by personal communication with author(s)

= calculated peak pressure from spatial-average temporal-average intensity (I_{SATA}) values obtained by personal communication with author(s).

Calculations were performed using the formulae (Kinsler, et al. 2000): $I_{SATA} = P^2/2\rho c$, where P denotes the peak pressure, and ρ and c denote the density and speed of sound, and $I_{SPTA} = I_{SATA}$/Duty factor